AD 431313

64-10

ASD-TR-61-445
PART III

THERMODYNAMICS OF INTERSTITIAL SOLID SOLUTIONS AND REFRACTORY COMPOUNDS

TECHNICAL DOCUMENTARY REPORT No. ASD-TR-61-445, PART III

NOVEMBER 1963

AIR FORCE MATERIALS LABORATORY
RESEARCH AND TECHNOLOGY DIVISION
AIR FORCE SYSTEMS COMMAND
WRIGHT-PATTERSON AIR FORCE BASE, OHIO

Project No. 7350, Task No. 735001

(Prepared under Contract No. AF 33(657)-9826 by
ManLabs, Inc., Cambridge, Massachusetts;
Larry Kaufman, Harold Bernstein and Ann Sarney, authors)

NOTICES

When Government drawings, specifications, or other data are used for any purpose other than in connection with a definitely related Government procurement operation, the United States Government thereby incurs no responsibility nor any obligation whatsoever; and the fact that the Government may have formulated, furnished, or in any way supplied the said drawings, specifications, or other data, is not to be regarded by implication or otherwise as in any manner licensing the holder or any other person or corporation, or conveying any rights or permission to manufacture, use, or sell any patented invention that may in any way be related thereto.

Qualified requesters may obtain copies of this report from the Defense Documentation Center (DDC), (formerly ASTIA), Cameron Station, Bldg. 5, 5010 Duke Street, Alexandria 4, Virginia

This report has been released to the Office of Technical Services, U.S. Department of Commerce, Washington 25, D.C., in stock quantities for sale to the general public.

Copies of this report should not be returned to the Aeronautical Systems Division unless return is required by security considerations, contractual obligations, or notice on a specific document.

200 - March 1964 - 162-29-553

FOREWORD

This report was prepared by the Research Division, ManLabs, Inc., under USAF Contract No. AF33(657)-9826. This contract was initiated under Project No. 7350 "Refractory, Inorganic Non-Metallic Materials", Task 735001 "Non-Graphitic". The work was administered under the direction of the A.F. Materials Laboratory, Research and Technology Division with Mr. Fred Vahldiek acting as project engineer.

This report covers the period of work from September 1962 to September 1963.

Personnel participating in the work included L. Kaufman, H. Bernstein, A. Sarney and L. Lindonen.

ABSTRACT

The thermodynamics of interstitial solid solutions and non-stoichiometric compounds have been applied to analyses of the Ti-C, Zr-C, Hf-C, Nb-C, Ta-C, Ti-O, Zr-O, Ti-N, and Zr-N systems. The thermodynamic framework, based on the Schottky-Wagner model for non-stoichiometric phases has been applied to predict phase equilibria and vaporization data for these systems. Comparison with experimental thermodynamic, vapor pressure, and equilibria data available in the literature is very satisfactory. In addition, correlation between thermodynamic properties and vacancy concentration data where possible yields good agreement. Results of x-ray measurements of the expansion coefficients and Debye temperatures of ZrC and HfC performed over the temperature range 25°C to 1500°C are also presented.

This technical documentary has been reviewed and is approved.

W. G. Ramke
Chief, Ceramics and Graphite Branch
Metals and Ceramics Division
AF Materials Laboratory

TABLE OF CONTENTS

LIST OF TABLES

LIST OF ILLUSTRATIONS

LIST OF ILLUSTRATIONS (Cont'd)

1.0 Introduction and Summary

During the past twenty years, increasing emphasis has been placed on the determination of the thermochemical properties of refractory compounds. As experimental research programs designed to yield information on the integral free energy of formation of these compounds developed, the experimental difficulties characteristic of such high temperature measurements became increasingly apparent. Moreover, the experience gained in performing reliable measurements, has yielded considerable insight into the costs of such investigations. Under these circumstances, it is quite apparent that a simple theoretical description of the thermodynamic properties of refractory compounds which could integrate the phase equilibria, vaporization, and integral free energies of compound phases would be extremely useful. The development of such a theoretical model, described in terms of explicit numerically predictable parameters, could be useful in correlating diverse data and in providing sound methods for estimating measurable quantities prior to the more expensive experimental studies.

The research reported in the body of this report describes the efforts made along these lines during the past year. The theoretical model chosen for simplicity, to describe the properties of NaCl type refractory carbide, oxide, and nitride phases was the Schottky-Wagner model which was first proposed about 30 years ago. This model has been applied for the specific case of a two-sublattice compound which might exist over a wide range of composition and temperature. By exploring the means of applying this model to the case at hand, it has been possible to integrate phase equilibria, vaporization information, and integral free energies of formation already available for refractory compound systems

---

Manuscript released by the authors 8 October 1963 for publication as an ASD Technical Documentary Report.

in addition to specifying direct numerical methods for predicting data which is presently not available. Although the present model is simple, possibly naive, it is explicit and offers a method for direct calculations.

The systems which have been considered are Ti-C, Zr-C, Hf-C, Nb-C, Ta-C, Ti-O, Zr-O, Ti-N and Zr-N. Although the present method of treating the stability of refractory compounds is not represented to be a panacea or a substitute for further experimental studies, its usefulness is quite apparent. Example comparisons of experimental and computed phase diagrams, vapor pressure vs. composition curves, congruent vaporization phenomena, and thermodynamic properties,detailed in this report, are quite encouraging.

A substantial part of Section 2 of this report will be published as a portion of a paper by Larry Kaufman and Edward V. Clougherty, entitled "Thermodynamic Factors Controlling the Stability of Solid Phases at High Temperatures and Pressures". This paper, which was presented at the Winter Meeting of the American Institute of Metallurgical Engineers in Dallas, Texas on 26 February 1963, will be published in a volume entitled "Metallurgy at High Temperatures and High Pressure" by AIME during 1964.

In addition to the thermodynamic investigation described above, x-ray studies of thermal expansion and lattice vibrations have been performed on ZrC and HfC. Measurements of Debye temperatures and coefficients of expansion for these compounds have been carried out at temperatures between 25°C and 1500°C using monochromatic radiation. The purpose of this study is to permit intercomparison between x-ray Debye temperatures and Debye temperatures derived from specific heat. These compounds were chosen for study because

of their practical interest and for the additional reason that while reliable low temperature specific heat data exist for ZrC no such data are presently available for HfC.

The x-ray results given in section 3.0 were used to estimate the vibration free energy of HfC and its contribution to the free energy of formation of HfC. The estimated free energy of formation of HfC is given as a function of temperature in TABLE IX. This latter information was used in the computation of phase equilibria (p 22) and vaporization (pp 29, 30, 36, and 37) in the hafnium-carbon system performed in section 2.0.

2.0 Thermodynamic Factors Controlling the Stability of Solid Phases at High Temperatures

Delineation of the thermodynamic factors controlling polymorphism in pure metals, and phase equilibria in binary substitutional metallic solutions has been accomplished with some success[1-5]. The purpose of this factorization is to predict and interpret high temperature phase equilibria in metallic systems[6-15].

In order to extend this approach to consideration of interstitial solid solutions and intermetallic compounds, it is necessary to perform an analogous factorization of energy-entropy terms and their respective concentration dependences which characterize these phase classifications. In particular, it is necessary to recognize the interaction between phase equilibria and free energy[16], and to formulate the free energy of compound phases in a manner which implicitly presupposes their "non-stoichiometric" nature[17].

Fortunately, statistical models for these situations have been presented in detail so that the present discussion need deal only with the application of these models to specific cases. Although these models are idealized, they offer a rational first approximation to the present problem. The Schottky-Wagner[18,19] model of non-stoichiometric phases will be used as the framework for describing the properties of compound phases, while the interstitial solutions will be described in terms of a model presented earlier[4].

As a final statement of introduction it is necessary to define the basis of the present discussion with reference to the size of the system and the reference states. Following the suggestions of Wagner[19] and Kubaschewski[20,21], it seems most convenient to restrict discussion to a system containing Avogadro's number, N, of atoms. Hence the mass basis is one gram atom of solution or

one gram atom of compound phase. Accordingly the composition of a given phase is specified by stating the atomic fractions of the component elements. Although this system is by no means universal it appears (in the opinion of the present authors) to be most convenient.

In concurrence with the viewpoint of Searcy[17], the reference states are chosen such that the free energies of the pure elements in their stable form at one atmosphere pressure and 0°K are zero. Although the choice of such a standard state is subjective, the present authors heartily endorse the suggestion that[17] "The usual thermodynamic convention of assignment of an activity of unity to the compound cripples efforts to understand the fundamental behavior of the system. The convention[19] of referral always to activities of the thermodynamic components of the compound, on the other hand, is a clear and uncomplicated framework of the detailed properties of the compound".

Since the symbolism of solution thermodynamics is by no means universal, a Table of Symbols is appended.

The simplest case to be considered along the lines discussed above is that of a binary system B-C in which there is a single compound existing over a range of composition near the equiatomic composition (i.e. $B_{0.5}C_{0.5}$) along with very little solubility of C in B or B in C. If in the temperature range of interest, the compound exhibits the σ crystal structure while B and C represent the β and γ structures respectively then the B-C phase diagram is exemplified by the Ti-C and Zr-C cases, where B stands for Ti and Zr, γ is the graphitic form of carbon, σ is the sodium chloride lattice arrangement, and x is the atomic fraction of carbon.

Figures 1 and 2 show current versions of the Ti-C[22] and Zr-C[23] phase diagrams as well as "calculated" or idealized phase diagrams for these systems. These "calculated" diagrams (which will be discussed in detail below) are not presented to correct or to cast doubt on the existing diagrams but rather to illustrate in a semi-quantitative way the relations between the free energies of the phases involved and the phase stability.

Figure 3 shows the integral free energy of ZrC as a function of composition at 2000°K. In addition Fig. 3 shows the partial molar free energies of zirconium and carbon, which are obtained graphically by tangent-intercept construction or mathematically from Eq. (A1-7). Fig. 3 has been calculated on the basis of the idealized model which will be discussed below. The lower panel of Fig. 3 shows the compositional variation of the partial free energies of zirconium and carbon across the ZrC σ field. Note the large variation with composition. If the pressure of zirconium over pure βZr (under atmospheric conditions) is p^{β}_{Zr} and the pressure of zirconium over ZrC of composition x is* $p^{\sigma}_{Zr}[x]$ then,

$$\bar{F}^{\sigma}_{Zr}[x] - F^{\beta}_{Zr} = RT \ln p^{\sigma}_{Zr}[x]/p^{\beta}_{Zr} \qquad (1)$$

where $\bar{F}^{\sigma}_{Zr}[x]$ is the partial molar free energy of zirconium at a composition x and F^{β}_{Zr} is the free energy of βZr. As indicated earlier the reference state is $F^{\alpha}_{Zr}[0^{\circ}K] = 0$. Similarly†

*In this paper, square brackets will be used to denote functional relations. Thus, $p^{\sigma}_{Zr}[x]$ is read the pressure of zirconium over the σ phase which is a function of composition.

†For purposes of the present discussion the higher polymers of gaseous carbon i.e. C_2, C_3, C_4, and C_5 etc., will not be considered in the present case although they are certainly important in the temperature range to be considered. Allowance for the association of gaseous carbon atoms can be made by utilization of available tabulations of thermodynamic functions[24-26] for the data of the free energies of association.

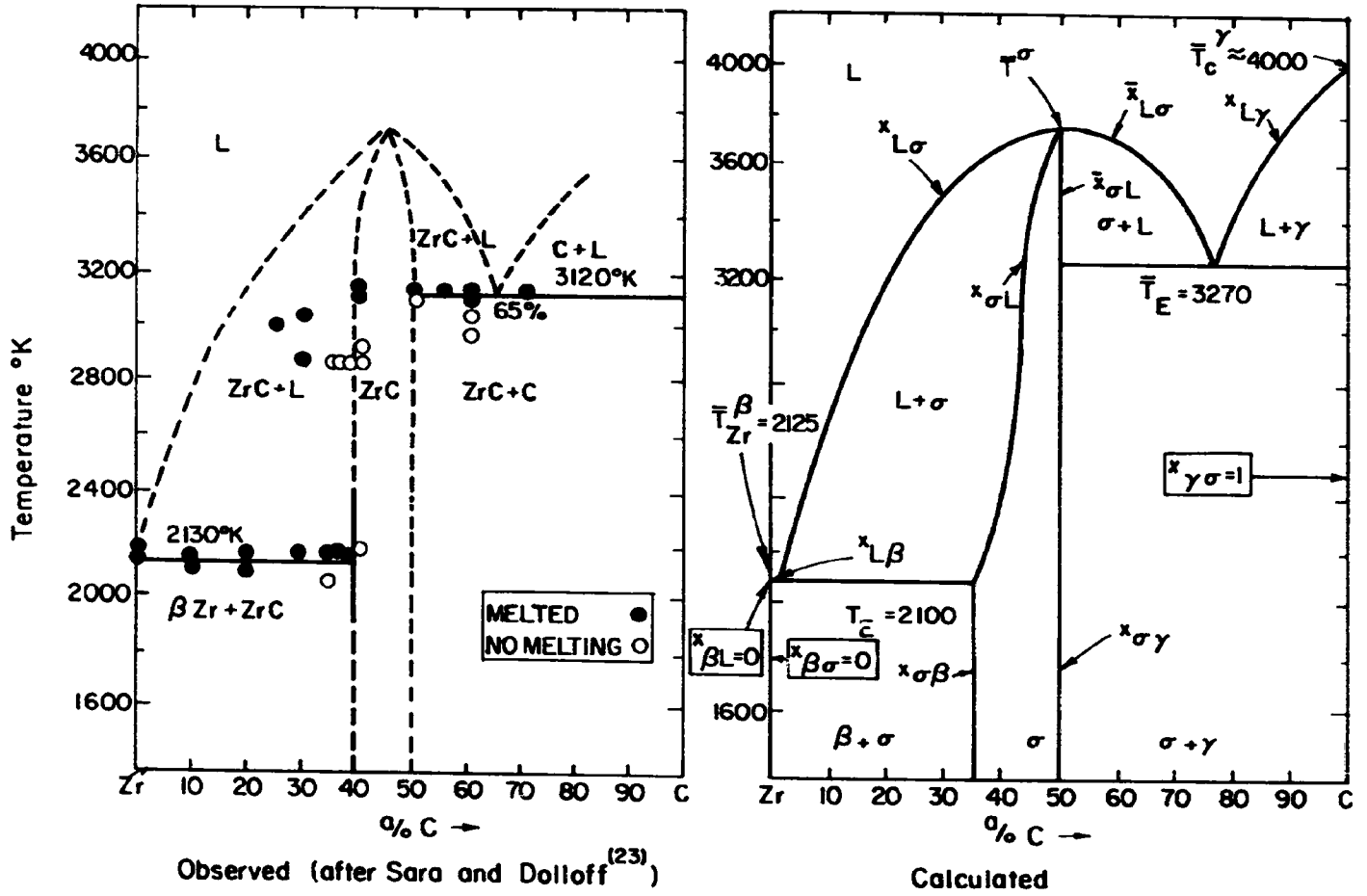

Fig. 1 — The Zirconium-Carbon phase diagram.

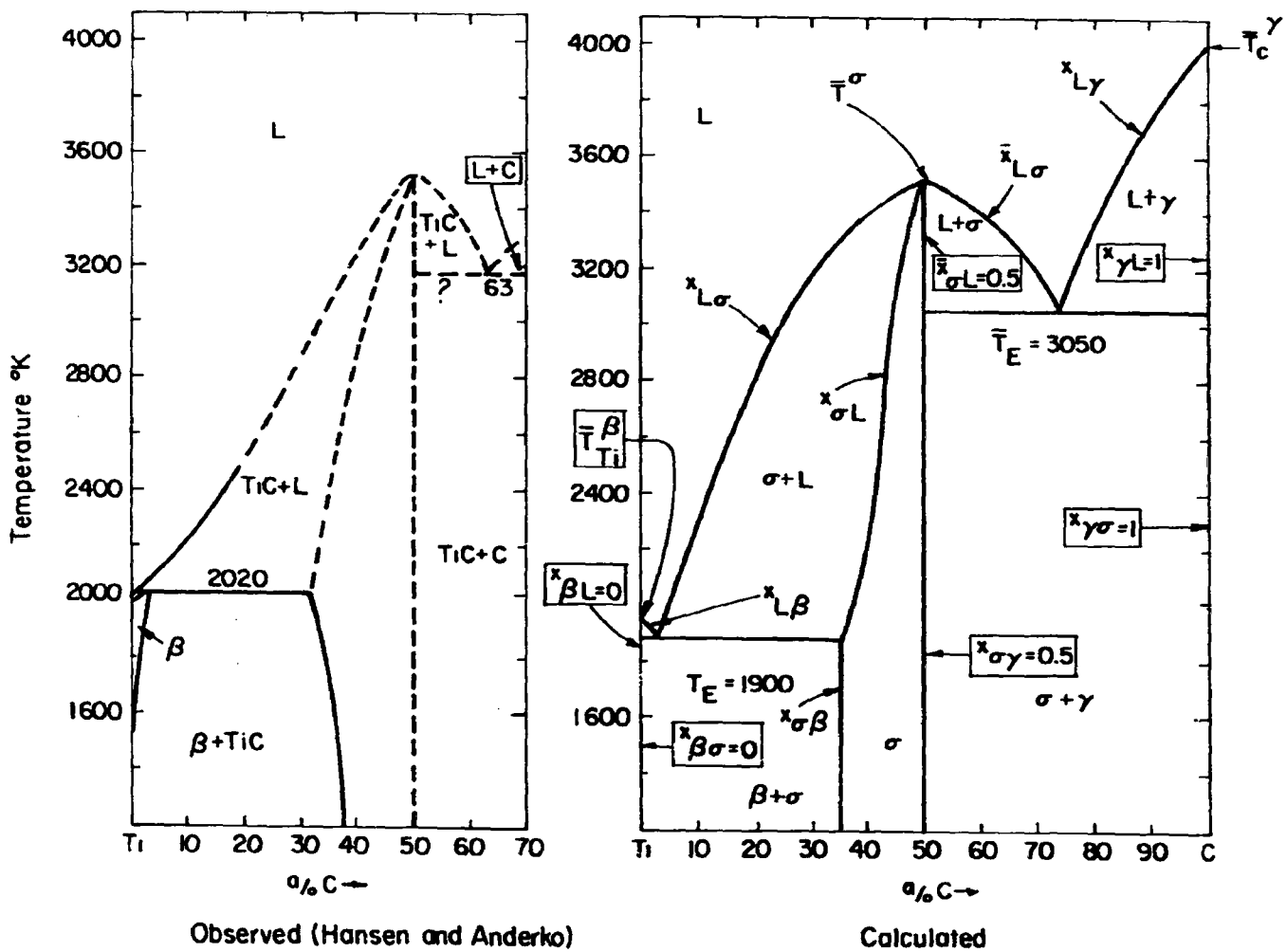

Fig.2 - The Titanium - Carbon phase diagram.

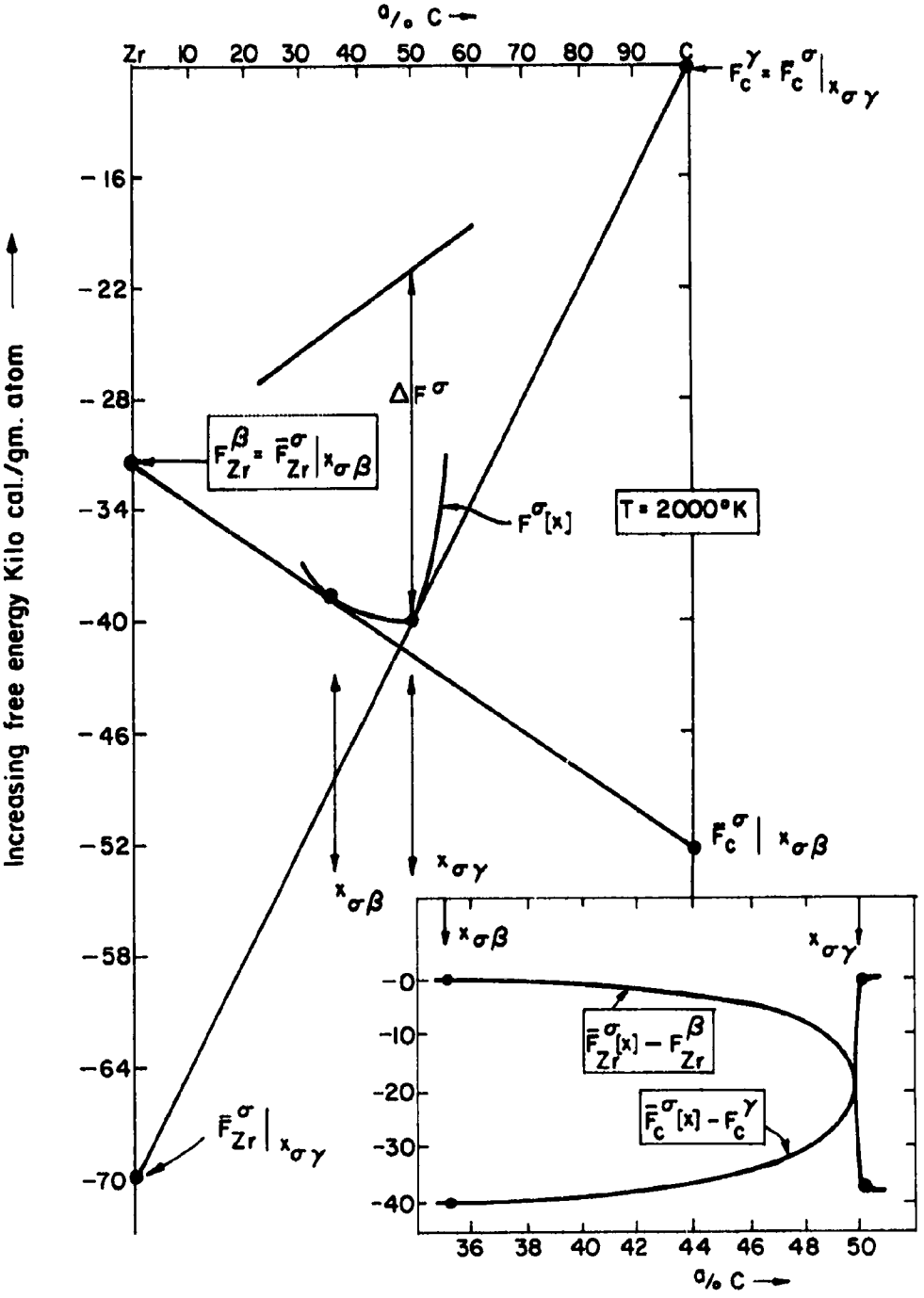

Fig. 3 – Calculated integral and partial free energy curves for the Zr-C system at 2000°K.

$$\overline{F}_C^{\sigma}[x] - F_C^{\gamma} = RT \ln p_C^{\sigma}[x]/p_C^{\gamma} \qquad (2)$$

Reference to Fig. 3 shows that a large variation of $p_{Zr}^{\sigma}[x]$, $p_C^{\sigma}[x]$, and the ratio $p_{Zr}^{\sigma}/p_C^{\sigma}$ (dropping the [x]) is to be expected across the σ field. Of particular interest is the composition of the free energy minimum where $\partial F^{\sigma}/\partial x$ equals zero. At this composition (Eq. A1-7), $\overline{F}_{Zr}^{\sigma} = \overline{F}_C^{\sigma}$. It should be noted that this composition need not coincide with the stoichiometric composition.

Figure 4 shows free energy-composition curves for the β, γ, σ and L (liquid phases) of the Zr-C system at temperatures above and below the melting point of Zr-C (which is assumed to occur at x = 0.5) and above and below the other invariant temperatures. These curves are idealized since they are based upon several simplifications which will be discussed in detail later but they should be illustrative of the general features of the real case. Fig. 4 shows the construction describing the free energy of formation of stoichiometric ZrC i.e. $\Delta F^{\sigma}[0.5]$ or ΔF^{σ}(dropping the [0.5]) in cal/g.atom. In this case $2\Delta F^{\sigma}$ is the free energy of formation in cal/mol which is the generally tabulated function[25,26]. Fig. 4 illustrates the graphical "common-tangent" construction which determines the phase boundaries. The mathematical equivalent of the common-tangent construction is the equilibration of the partial molar free energies of both components across the two phase field. For example at T = 3400°K in the ZrC system (Figs. 1 and 4) the partial molar free energy of zirconium in the liquid phase at a composition $x_{L\sigma}$ is equal to the partial molar free energy of zirconium in the σ phase at a composition $x_{\sigma L}$ and a similar equation holds for carbon atoms. Mathematically,

$$\overline{F}_{Zr}^{L}\Big|_{x_{L\sigma}} = \overline{F}_{Zr}^{\sigma}\Big|_{x_{\sigma L}} \qquad (3)$$

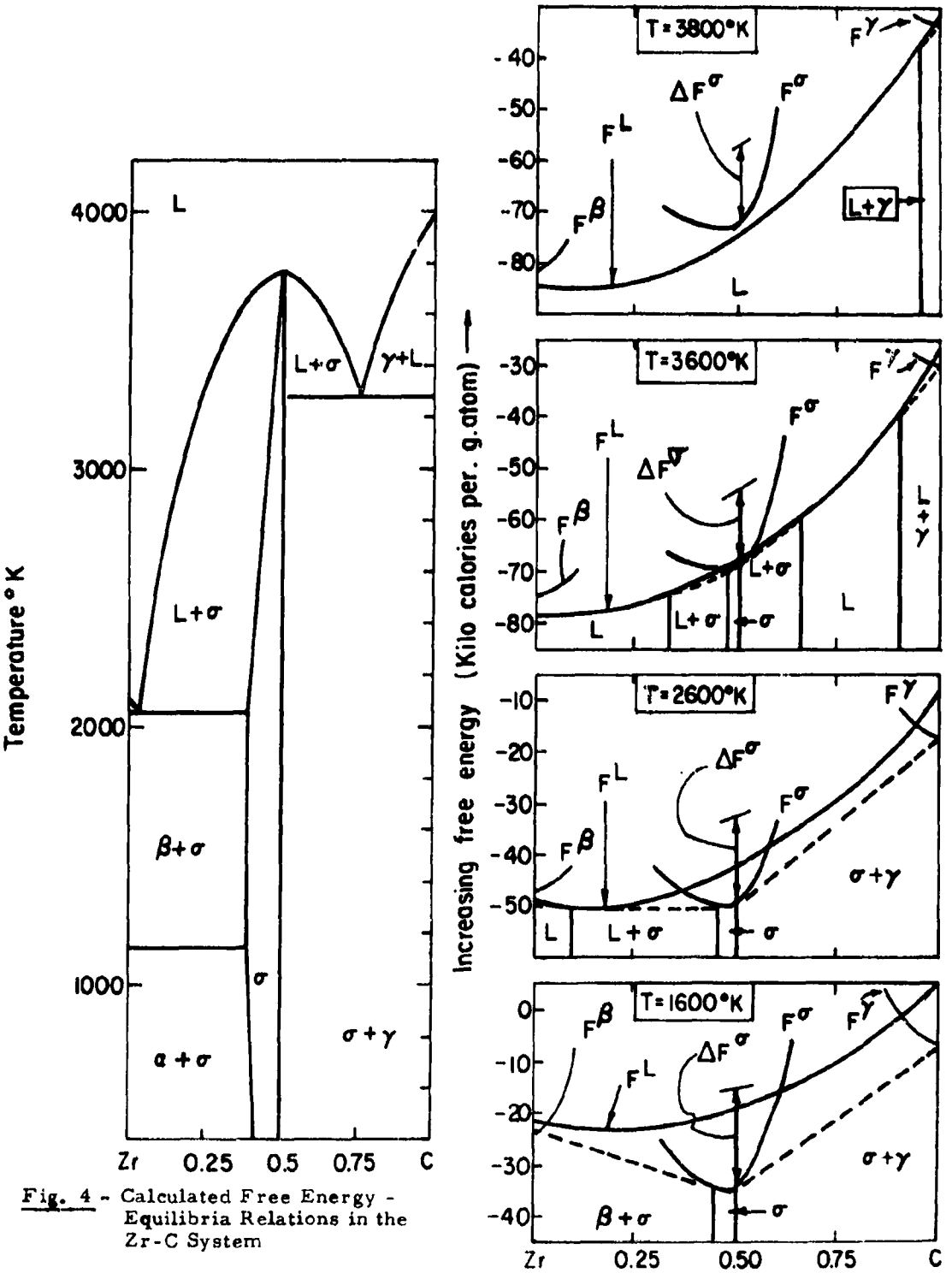

Fig. 4 - Calculated Free Energy - Equilibria Relations in the Zr-C System

and $$\overline{F}_C^L\big|_{x_{L\sigma}} = \overline{F}_C^\sigma\big|_{x_{\sigma L}} \qquad (4)$$

Eqs. 3 and 4 are the equivalent of the rule of "common-tangents".

One of the general features of Fig. 4 which does not depend upon models or approximations are the relative magnitudes of ΔF^σ, F_C^γ, and F_{Zr}^β as functions of temperature. Since the entropy of zirconium is much larger than that of carbon at any temperature it has a much lower free energy. Coupling this fact with the known compositional limits of the σ phase (i.e. $\overline{x}_{\sigma\gamma} = 0.5$ and $x_{\sigma\beta}$ less than 0.5) require that the composition at which F^σ is a minimum must be located at $x \leq 0.5$.

In order to inquire more deeply into the factors determining the temperature and compositional range of stability of compound phases it is necessary to consider the "shape" of the free energy vs. composition curve (i.e. as shown in Fig. 3) and the factors which determine the shape in the vicinity of the minimum. Such considerations are best demonstrated by discussing specific examples. The examples which will be discussed in subsequent portions of this section are the

a. Ti-C, Zr-C, Hf-C, Nb-C, and Ta-C systems
b. the Ti-O and Zr-O systems
c. the Ti-N and Zr-N systems

As indicated earlier, the consideration of these systems will be made on on the basis of the Schottky-Wagner model in whose context these cases (a, b, and c) represent three distinct classes. In some respects however, these systems are similar since all the compounds of interest are refractory phases of the sodium chloride type which exist over a range of composition near $x = 1/2$*.

*The Zr-O system does not exhibit the sodium chloride $x = 1/2$ structure.

Similar analyses can be applied to other phase classifications having different crystal structures corresponding to other stoichiometric compositions. The difficulties in dealing with other stoichiometries (i. e. 1/3, 1/4, 2/5 etc.) are algebraic rather than conceptual (See Appendix A1).

Although a detailed description of the particular variant of the Schottky-Wagner model used in the present considerations is given in Appendix A1 it is of value to present the reader with a qualitative, quasi-physical description of the model before launching into a detailed application to specific systems. The best point of departure for such a consideration is the vacancy parameter α which is directly proportional to the fraction of vacant lattice sites at stoichiometry. For the case of 50/50 compounds 2α is the fraction of metal (or non-metal) lattice points which are vacant. If α is very small i. e. less than 0.1% then (for 50/50 compounds)

$$2\Delta F^{\sigma}[x=0.5] = -F_{Me+} - F_{C+} - 2\ RT\ \ln 2\alpha \qquad (5)$$

where ΔF^{σ} is the free energy of formation of the stoichiometric compound in cal/g. atom. In Eq. (5), F_{Me+} and F_{C+} are the free energies of formation of metal and carbon vacancies in the compound. Consequently, three new parameters, F_{Me+}, F_{C+}, and α are introduced and interrelated through Eq. (5). These parameters control the "shape" of the free energy curve near its minimum point. Thus, on the metal rich side of stoichiometry there is an excess of C vacancies and the rate of ascent of the F^{σ} vs x curve will depend on the magnitude of F_{C+}. On the carbon rich side the reverse is the case. Since the partial free energies in a sense reflect the compositional variation of $F^{\sigma}[x]$ they are determined by by F_{Me+}, F_{C+}, and α.

Finally, Eq.(5) states that for a given free energy of formation, the fractional number of vacancies will depend upon the free energy of formation of metal and carbon vacancies. This equation is obtained by writing a general equation for the free energy of a gram atom of compound of a fixed composition at a fixed temperature and pressure. This compound is envisioned to contain an arbitrary number of metal and non-metal vacancies which contribute positive free energy increments through F_{Me+} and F_{C+} and negative free energy increments via the entropy of mixing. The overall free energy is then minimized (at constant temperature, pressure and composition) by allowing the number of vacancies to vary, yielding equation (5) as the criterion for minimum free energy.

2.1 Discussion of the Ti-C, Zr-C, Hf-C, Nb-C and Ta-C Systems

In order to proceed with the discussion of the metal-carbon systems, it is necessary to consider the properties of the graphite form of carbon, C^{γ}, which sublimes at about $4000^{\circ}K$[26]. By combining the thermodynamic data for C^{γ} with the entropy[20] and enthalpy[20] of the diamond form of carbon, C^{δ}, at ($298^{\circ}K$) and the high temperature data[26,27] for C^{δ} and C^{γ}, the free energy difference between δ and γ can be approximated (for $T > 400^{\circ}K$) as

$$\Delta F_C^{\delta \rightarrow \gamma} = -280 - 1.16T \text{ cal/g.at.} \qquad (6)$$

Since the volume change at room temperature can be computed from the volume per gram atom of graphite[28] and diamond[29] as $\Delta V_C^{\delta \rightarrow \gamma} \sim +1.91$ cm^3/g.at. The pressure dependence of Eq(6) can be approximated as[8]

$$\Delta F_C^{\delta \rightarrow \gamma}[T,P] \simeq -280 - 1.16\,T + 23.9\,P(1.91) \text{ cal/g.at.} \qquad (7)$$

where P is the pressure in kilobars*.

*Note that the factor 23.9 in Eq.(7) is a factor converting kilobars to cal/cm^3.

Setting Eq. (7) equal to zero gives a reasonably good calculation of the T-P curve for the $\gamma \rightleftarrows \delta$ conversion line [30, 31].

The entropies of melting of the diamond cubic forms of Si, Ge, and Sn[8] are 6.6, 6.3, and 5.3 cal/g.at. °K respectively. Therefore the entropy of melting of diamond might be expected to be about 6 cal/g.at. °K. Combination of this estimate with the entropy change for the $\delta \rightarrow \gamma$ reaction (Eq. 6) results in an estimated value of 5 cal/g. at °K for the entropy of melting of graphite. Bundy[30] has measured the enthalpy of melting of C^{γ} at high pressures and temperatures and suggests that $\Delta S_C^{\gamma \rightarrow L} \approx 5.4$ cal/g.at. Since the γ-L- vapor triple point occurs at about 0.11 kbars and 4000°K[31, 32] it is safe to estimate the melting point of graphite, i.e. $\overline{T}_C^{\gamma}$, as about 4000°K. Hence

$$\Delta F_C^{\gamma \rightarrow L} \approx 21,600 - 5.4T \text{ cal/g.at.} \qquad (8)$$

Although this expression is slightly in error due to the fact that $\overline{T}_C^{\gamma}$ must be higher than the sublimation temperature (since graphite sublimes at atmospheric pressure and 4000°K) examination of the available data[31, 32] indicates that the difference in temperature between the melting point and sublimation point is not large.

In order to calculate the Zr-C and Ti-C phase diagrams the following assumptions are made (See Figs 1 and 2)

a. $x_{\beta\sigma}$ and $x_{\beta L} = 0$, $x_{\gamma\sigma}$ and $x_{\gamma L} = 1$, and $x_{\sigma\gamma}$ and $x_{\sigma L} = 0.5$

b. The melting point of the σ phase occurs at $x = 0.5$

These "idealizations" are not too far from reality and are used to simplify the arithmetic. Finally a more questionable assumption is made concerning the properties of the liquid phase i.e. that it is regular. Hence,

$$F^L = (1-x)F^L_{Me} + xF^L_C + RT\,(x\ln x+(1-x)\ln(1-x)) + Lx(1-x) \qquad (9)$$

where L is a constant. The only palatable feature of this assumption is that L is directly specified since at $x=0.5$ and $T=\overline{T}^\sigma$, $F^L=F^\sigma$. Assuming that α is a small number (i.e. that $\Delta F^\sigma[0.5,T] \sim \Delta F^\sigma_*$ (see Table A1-I))

$$L = 4\,(\Delta F^\sigma[\overline{T}^\sigma] + \overline{T}^\sigma R\ln 2 + 0.5\Delta F^{L\rightarrow\gamma}_C[\overline{T}^\sigma]) \qquad (10)$$

Using the tabulated values[26] for $\Delta F^\sigma[T]$ (in cal/g.at.), Eq.(7), and the published melting points 3750°K, 3520°K, and 4070°K one obtains $L = -36,080$, $-44,620$, and $-42,780$ cal/g.at. respectively for the Zr-C, Ti-C, and Ta-C cases.

Next, advantage is taken of the fact that $x_{\sigma\gamma}=0.5$, and $x_{\gamma\sigma}=1$. Since equilibration across the $\sigma+\gamma$ field requires that

$$\overline{F}^\gamma_C\big|_{x_{\gamma\sigma}} = \overline{F}^\sigma_C\big|_{x_{\sigma\gamma}} \qquad (11)$$

Then (Eq. A1-10)

$$F_{C+} = -RT\ln 2\alpha \qquad (12)$$

The $x_{L\sigma}$ and $\overline{x}_{L\sigma}$ vs T curves can now be calculated. On the basis of Eqs. 9, 10, and (A1-7),

$$\overline{F}^L_{Me} = F^L_{Me} + RT\ln(1-x) + Lx^2 \qquad (13)$$

and

$$\bar{F}_C^L = F_C^L + RT \ln x + L(1-x)^2$$

Equilibrating the partials across the $L + \sigma$ fields for $\bar{T}_{Me}^{\beta} < T < \bar{T}_C^{\gamma}$ (and using Eqs. A1-11-14) yields

$$2\Delta F^{\sigma} + \Delta F_C^{L\to\gamma} = RT \ln(1-x_{L\sigma})x_{L\sigma} + L((1-x_{L\sigma})^2 + x_{L\sigma}^2) + RT \ln(1-x_{\sigma L})x_{\sigma L}^{-1} \tag{14}$$

and

$$2\Delta F^{\sigma} + \Delta F_C^{L\to\gamma} = RT \ln(1-\bar{x}_{L\sigma})\bar{x}_{L\sigma} + L((1-\bar{x}_{L\sigma})^2 + \bar{x}_{L\sigma}^2) \tag{15}$$

where ΔF^{σ} and $\Delta F_C^{L\to\gamma}$ are understood to be temperature dependent. Since the last term on the right of Eq. 14 is small enough to be neglected in the first approximation, Eqs. (14) and (15) can be used to calculate $x_{\sigma L}$ and $\bar{x}_{\sigma L}$. For temperatures below $\bar{T}_{Me}^{\beta}$, $\Delta F_{Me}^{L\to\beta}$ must be added to the left side of Eq. (14). This quantity is approximately equal[26] to $-2.3\,(\bar{T}_{Me}^{\beta} - T)$.

The calculation of the $x_{\beta L}$ vs T curve is made by equilibrating the metal partials across the $\beta + L$ field hence,

$$\Delta F_{Me}^{L\to\beta} = RT \ln(1-x_{L\beta}) + L x_{L\beta}^2 \tag{16}$$

Similarly the $x_{L\gamma}$ vs T curve results from

$$\Delta F_C^{L\to\gamma} = RT \ln x_{L\gamma} + L(1-x_{L\gamma})^2 \tag{17}$$

The eutectics T_E and $\bar{T}_E$ result from the intersection of the $x_{L\beta}$ and $x_{L\sigma}$ curves and the $x_{L\gamma}$ and $\bar{x}_{L\sigma}$ curves since at T_E, $x_{L\beta} = x_{L\sigma}$ while at $\bar{T}_E$, $x_{L\gamma} = \bar{x}_{L\sigma}$. Assumption a) above requires the occurrence of eutectics. If this assumption is relaxed (complicating the arithmetic) then peritectics can occur.

Up to this point no assumptions concerning the σ phase have been made other than $x_{\sigma\gamma} = 0.5$ which leads to Eq. (12). In order to complete the calculation of the diagram, an additional "post facto" assumption concerning the σ phase is required. This additional assumption is made by setting

$$RT \ln \alpha = 2\Delta H^{\sigma}[0^{\circ}K] \tag{18}$$

where $\Delta H^{\sigma}[0^{\circ}K]$ is the enthalpy of formation (cal/g. at.) of the compound at $0^{\circ}K$. This assumption fixes F_{C+}, (Eq. 12), and F_{Me+}, (Eq. 5),

$$F_{Me+} = -2\Delta H^{\sigma}[0^{\circ}K] - RT \ln 2 - 2\Delta F^{\sigma}[T] \tag{19}$$

For the Zr-C case at $2000^{\circ}K$, substitution of the tabulated values[26] yields $F_{Zr+} = 79,750$, $F_{C+} = 41,350$, and $RT \ln \alpha = -44,100$ cal/g. atom respectively. Thus, α is a very small number (i.e. about 10^{-5}) and F_{Zr+} is much larger than F_{C+} leading to the asymmetry in the F^{σ} vs. x curves shown in Figs. 3 and 4. With this assumption, the $x_{\sigma\beta}$ and $x_{\sigma L}$ curves can be calculated by equilibrating the partials of the metal atom across the $\beta + \sigma$ and $\sigma + L$ fields. The results are

$$RT \ln (1-2x_{\sigma\beta})/(1-x_{\sigma\beta}) = 2\Delta H^{\sigma}[0^{\circ}K] - 2\Delta F^{\sigma}[T] + RT \ln 2 \tag{20}$$

for $T < T_E$ yielding $x_{\sigma\beta}$ vs T. The calculation of $x_{\sigma L}$ is made in the same manner for $T > T_E$ from Eq. (21)

$$RT \ln (1-2x_{\sigma L})/(1-x_{\sigma L}) = 2\Delta H^{\sigma}[0^{\circ}K] - 2\Delta F^{\sigma}[T] + RT \ln 2 + RT \ln (1-x_{L\sigma}) + x_{L\sigma}^2 L \tag{21}$$

for $T > T_{Me}^{\beta}$. If $T_{Me}^{\beta} > T > T_E$, $\Delta F_{Me}^{\beta \rightarrow L}$ must be added to the right side of Eq. (21). Since $x_{L\sigma}$ vs. T is known from Eq. (14) at this point, then $x_{\sigma L}$ vs. T is defined. These $x_{\sigma L}[T]$ values can be resubstituted into Eq. (14) to reiteratively recalculate $x_{L\sigma}[T]$.

Briefly then, Figs. 1-4 result from assumptions a) and b), and the ad hoc assumptions of regularity for the liquid phase and Eq. (18) describing the vacancy concentration of the σ phase. Needless to say these equations can be applied to calculate any of the other metal-carbon phase diagrams which are suspected to have similar features i.e. Hf-C, Nb-C, V-C, etc. This might be a useful first approximation in cases where phase diagram data are absent or sketchy. In addition these equations can be used to calculate the activity and vapor pressure (i.e. Fig. 3) across the single phase σ field.

Fig. 5 shows the calculated Ta-C phase diagram, with the calculation performed as if Ta_2C is non-existent. Consequently, the modification which might be expected if Ta_2C is included is shown by adding the full lines. The observed Ta-C diagram shows the Ta_2C peritectic near 3700°K. At this temperature the calculated value of $x_{L\sigma}$ is about 0.33 so that $F^{L}[0.33]$ should be approximately equal to the free energy of Ta_2C at this temperature. Performing this calculation yields a free energy of formation of Ta_2C at 3700°K as -28,250 cal/g.at. while the tabulated value[26] is -29,100 $\pm$ 2500.

Apart from using this formalism to develop semi-quantitative expressions for the partial free energies, the representation of the composition dependencies of the vapor pressure can be used in some kinetic considerations. For example the rate of Langmuir evaporation, G, is given by

$$G = 44.4\, p\, M^{-1/2} T^{-1/2} \text{ mols/cm}^2\text{sec} \qquad (22)$$

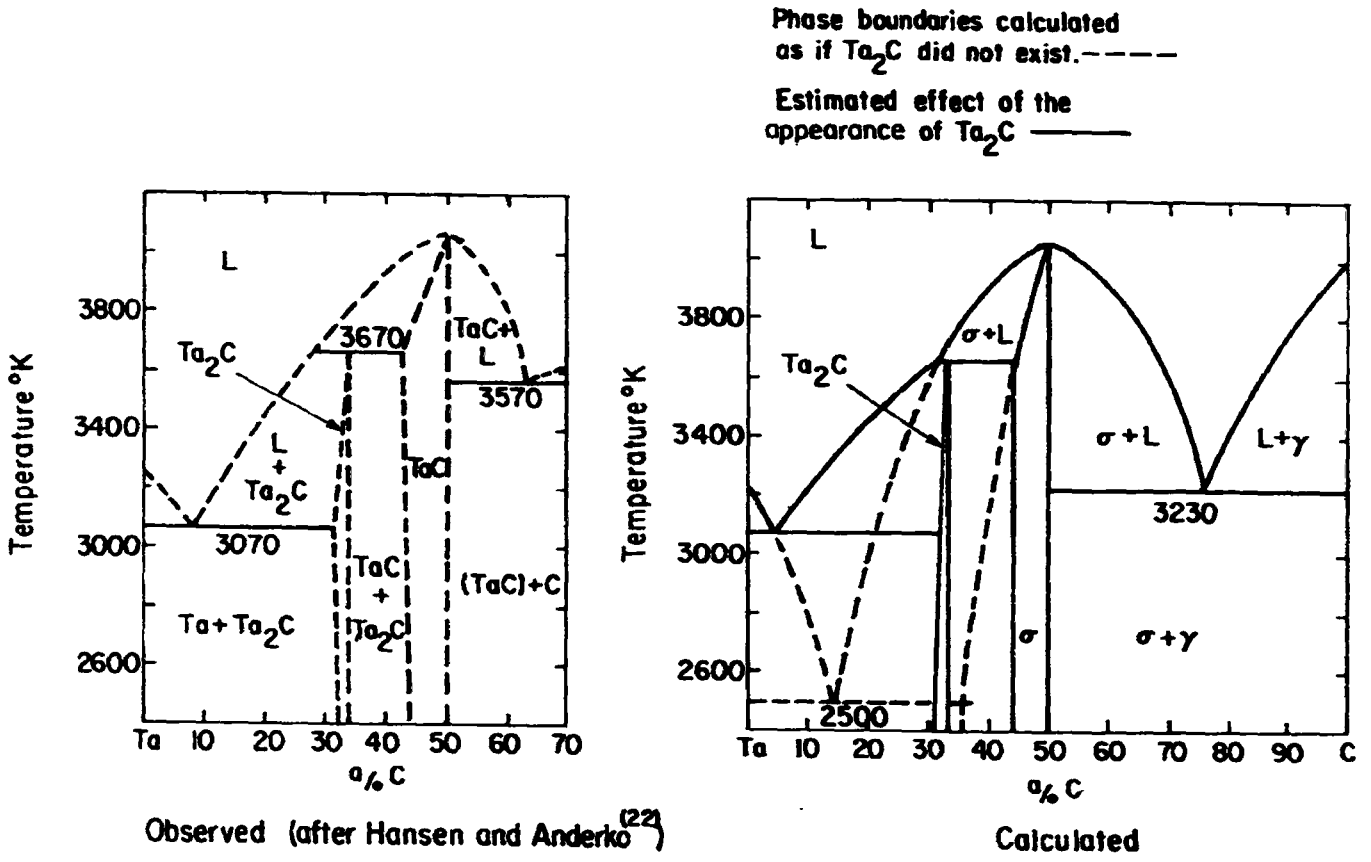

Fig. 5— The Tantalum—Carbon phase diagram.

The composition at which congruent vaporization occurs at a given temperature x_c, is defined by the condition

$$G_C/G_{Me} = x_c/(1-x_c) \tag{23}$$

or

$$p^{\sigma}_C[x_c]/p^{\sigma}_{Me}[x_c] = x_c(1-x_c)^{-1}M_{Me}^{-1/2}M_C^{+1/2} \tag{24}$$

Since $p^{\sigma}_C[x_c]/p^{\sigma}_{Me}[x_c]$ can be calculated as a function of composition, x_c vs. T can also be calculated (see Fig. 3).

Equations, 1, 2, 5, 12, 18, 19, A1-9 through 12, of Appendix AI and the known vapor pressures of pure carbon, Ti, Zr, Hf, Nb, and Ta tabulated by JANAF can be employed to predict the vapor pressures of metal and carbon over the refractory carbides. The pertinent results are:

$$RT \ln p^{\sigma}_{Me}[0.5]/p^{o}_{Me} = -F_{Me+} - RT \ln 2\alpha$$

$$RT \ln p^{\sigma}_{C}([0.5]/p^{o}_{C} = -F_{C+} - RT \ln 2\alpha$$

for $x = 0.5$ i.e. at the stoichiometric composition, and

$$RT \ln p^{\sigma}_{Me}[x]/p^{o}_{Me} = -F_{Me+} + RT \ln (1-2x)\, 4^{-1}(1-x)^{-1}\alpha^{-2}$$

$$RT \ln p^{\sigma}_{C}[x]/p^{o}_{C} = -F_{C+} + RT \ln x(1-2x)^{-1}$$

when x is less than 0.5. These equations can be applied to the refractory NaCl type monocarbide phases in the Ti-C, Zr-C, Hf-C, Ta-C and Nb-C systems, since the free energy of formation at stoichiometry $\Delta F^{\sigma}[0.5]$ is known. Note that these are the same equations used in computing the binary phase diagrams shown in Figs. 1-5. The following sources were used for $2\Delta F^{\sigma}[0.5]$; TiC and ZrC (Elliot and Gleiser, Thermochemistry for Steelmaking Addison-Wesley Publishers, Reading, Mass., 1960): -32,300 + 1.32T cal/mol for NbC and -35,900 + 1.2T cal/mol for TaC (both from W. Worrel, ScD Thesis, M.I.T.,*

*(Submitted for publication to J. Physical Chemistry by W. Worrell and J. Chipman, Oct. 1963. In the publication version, the authors modified the NbC equation to -31,800 + 1.6T and the TaC equation to -35,600 + 1.6T. These modifications will produce minor changes in Figs. 12-15).

May'63): and $2\Delta F^{\sigma}[0.5]$ for HfC as given in TABLE IX*.

These calculations can be performed explicitly at any temperature desired and are shown in Figs., 6 through 15 at selected temperatures. These curves depict, in explicit fashion, the vapor pressures of both components over the single phase refractory carbide field.

Since the rate of Langmuir evaporation (Eq. 22) can be expressed in terms of the vapor pressure, these equations or curves can be used to predict rates of evaporation. Crossing of the component pressure vs. composition curves (which occurs for ZrC and HfC) indicates congruency. Application of Eqs. (23) and (24) yields

$$2\,RT\ln(1-2x_c) = RT\ln p_C^o/p_{Me}^o - 0.5\,RT\ln M_C/M_{Me} - F_{C+} + F_{Me+} + 2\,RT\ln\alpha \qquad (25)$$

where x_c is the composition for congruent vaporization and M_C and M_{Me} the atomic weights of carbon and metal respectively. Equation (25) explicitly defines x_c. Once x_c is calculated (as a function of temperature), then $p_{Me}^{\sigma}[x_c, T]$ and $p_C^{\sigma}[x_c, T]$ which are the pressures of metal and carbon at the congruently vaporizing composition as a function of temperature can be predicted. These curves, predicted for ZrC and HfC are compared in Figs. 16 to 19 with measurements at G.E. For TiC, where congruency is not indicated by Figs. 6 and 7, the rate of evaporation of carbon saturated TiC (i.e. $x = 0.5$) has been calculated and compared with measurements in Fig. 20. Excellent agreement is obtained. For the TaC and NbC cases, there are no vapor pressure data available to compare with the predicted pressure composition curves. However, E.K. Storms and N.H. Krikorian (J. Phys. Chem. (1960) 64 1471) indicate that in niobium carbide at

*In the calculated Hf-C phase diagram (i.e. similar to Figs 1, 2 and 5 with $T_{Hf} = 2495^{\circ}K$, $T^{\phi} = 4170^{\circ}K$) the HfC-C eutectic is calculated at $3100^{\circ}K$ and $78^{a}/oC$ while the HfC-Hf eutectic is calculated at $2200^{\circ}K$ and $7^{a}/oC$. At this temperature the Hf rich boundary of HfC is computed at $36^{a}/oC$.

3070°K, congruent vaporization occurs at a composition of 41.5 atomic percent carbon. The predicted value (i.e. see Fig. 13) is about 40%.

In addition to the demonstrated value of the present approach in dealing with the prediction of phase equilibria and vaporization, there is an additional area of importance to which it can be applied. Berkowitz (ASD Technical Report #62-203 pt II January, 1963 "Kinetics of Oxidation of Refractory Metals and Alloys at 1000°C-2000°C" pp 26-68) has applied the Webb, Norton, and Wagner theory of oxidation to a consideration of the oxidation resistance of group IVA, VA, and VIA metal carbides. Dr. Berkowitz has shown that this theory can usefully predict an upper limit to the temperature at which these carbides can be applied. In order to apply the WNW theory (pp 27-29, Eqs. II-1 through II-9 of TR #62-203), it is required that thermodynamic data on the activity of carbon and metal in the compound at the composition in question be available. The actual numerical values of $a_C^{\sigma}[x]$ and $a_{Me}^{\sigma}[x]$ play an important role in controlling the vapor pressure of volatile oxidation products whose formation limits the operating temperature.

Thus, the application of the Schottky-Wagner model provides an idealized but explicit framework for integrating the equilibrium and vaporization properties of the carbides. The method should not be construed as a replacement for experimental research, but rather as a guide for performing the extremely difficult high temperature equilibria measurements. Moreover, if suitably extended to the three component case, it can be used to make intelligent estimates of ternary equilibria and vaporization.

A final point of application of this method is in the consideration of metastable equilibrium. To illustrate this point, consider Fig. 5, which shows the calculated Ta-C phase diagram ignoring Ta_2C. The predicted eutectic at 2500°K

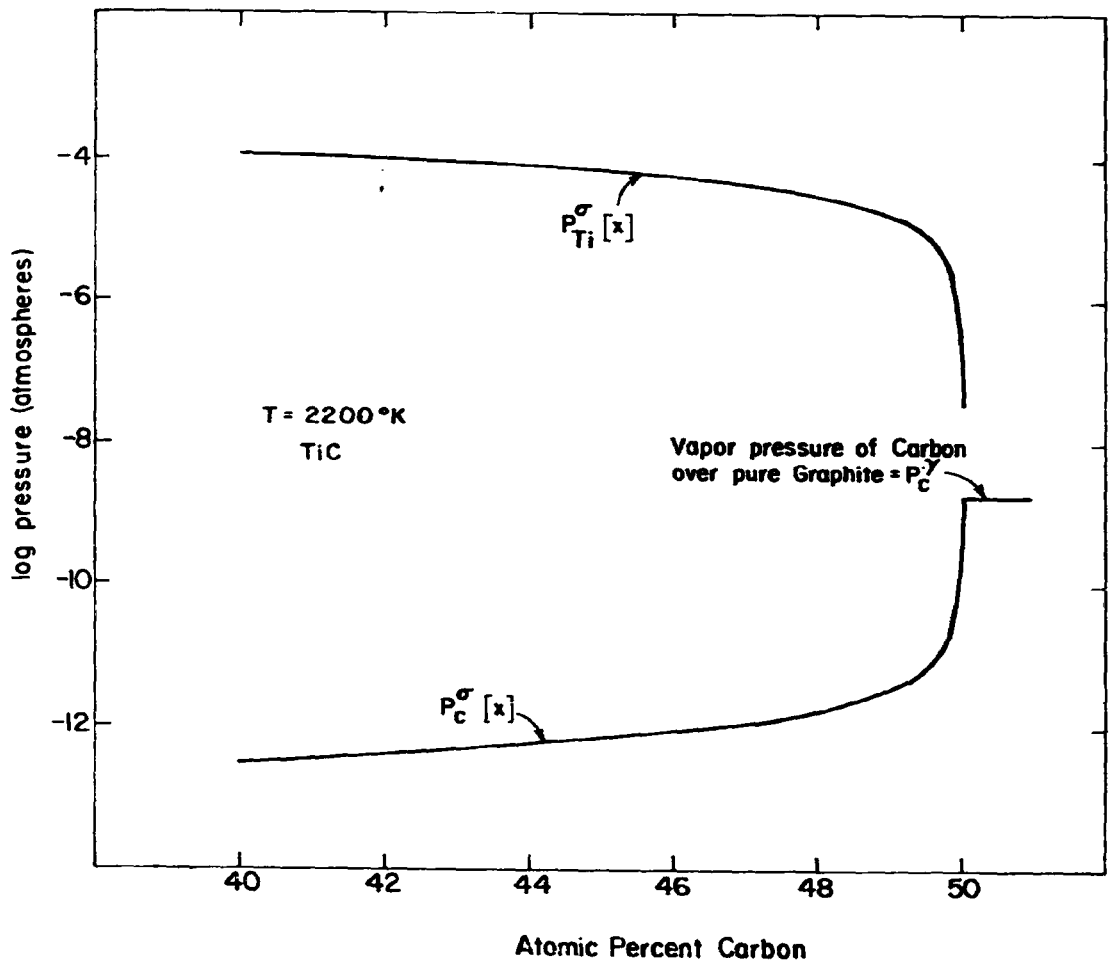

Fig. 6 - Calculated compositional dependence of the vapor pressures of Ti and C over the TiC$^{\sigma}$ phase at 2200°K.

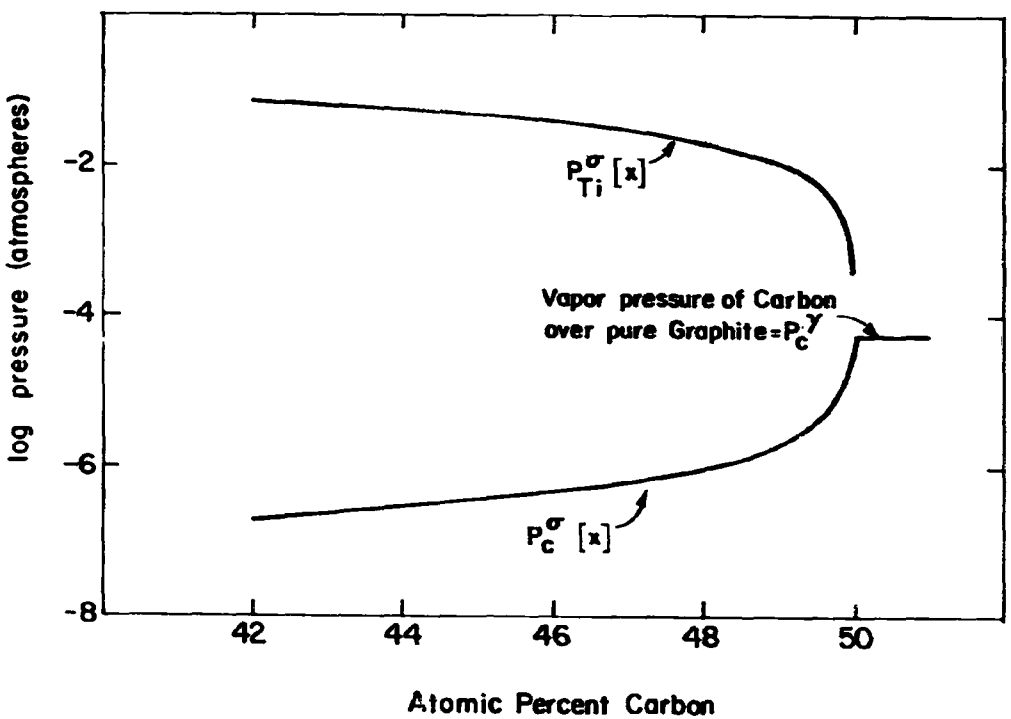

Fig. 7 - Calculated compositional dependence of the vapor pressures of Ti and C over the TiC^{σ} phase at 3000°K.

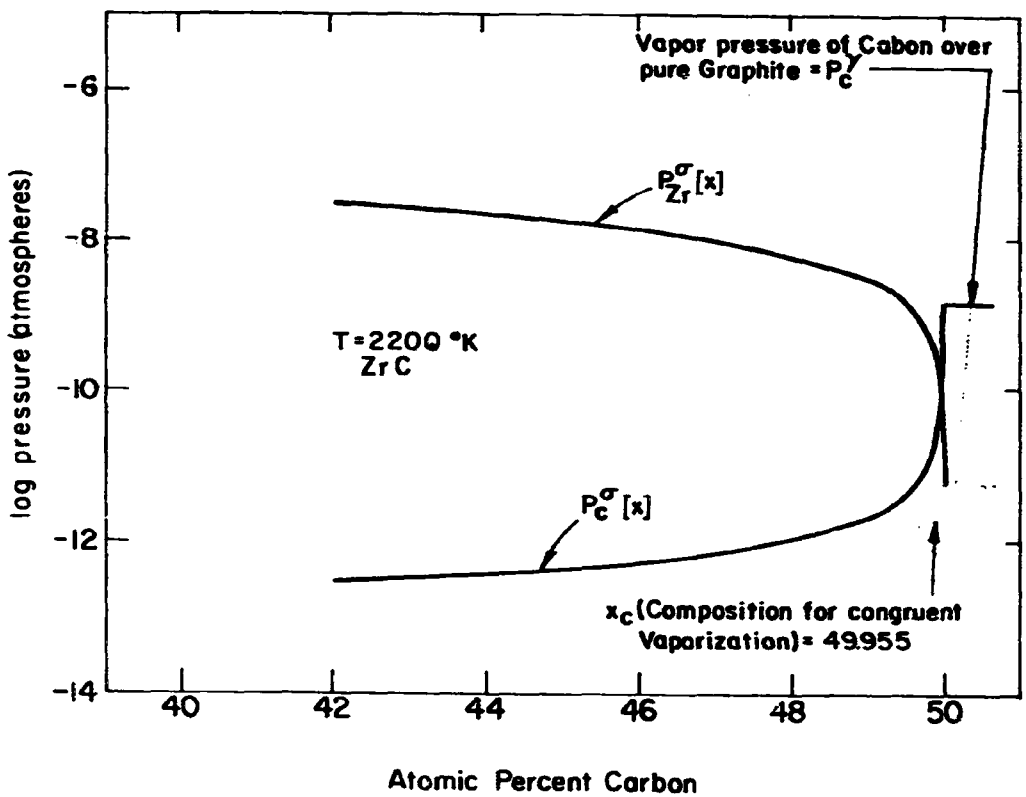

Fig. 8 - Calculated compositional dependences of the vapor pressure of Zr and C over the ZrC^σ phase at 2200 °K.

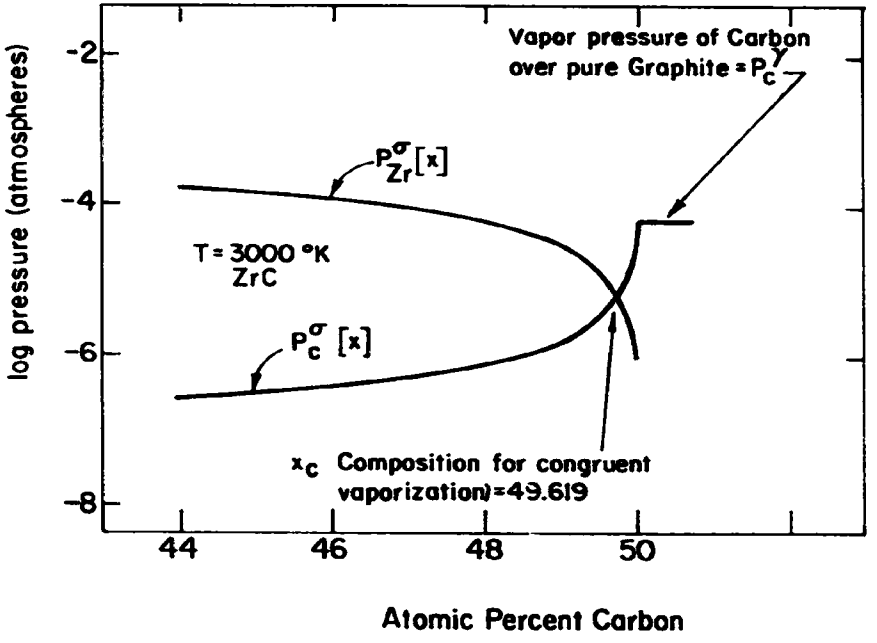

Fig. 9 - Calculated compositional dependence of the pressure of Zr and C over the ZrC^σ phase at 3000 °K.

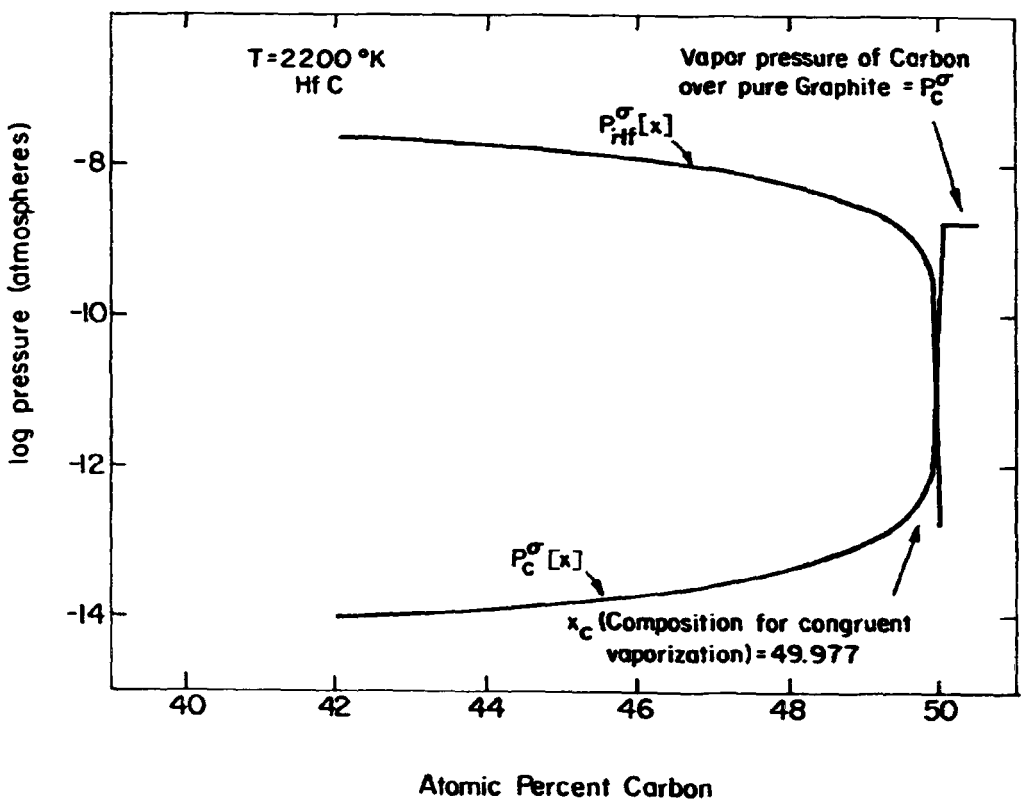

Fig. 10 - Calculated compositional dependence of the vapor pressure of Hf and C over the Hf C^σ phase at 2200°K.

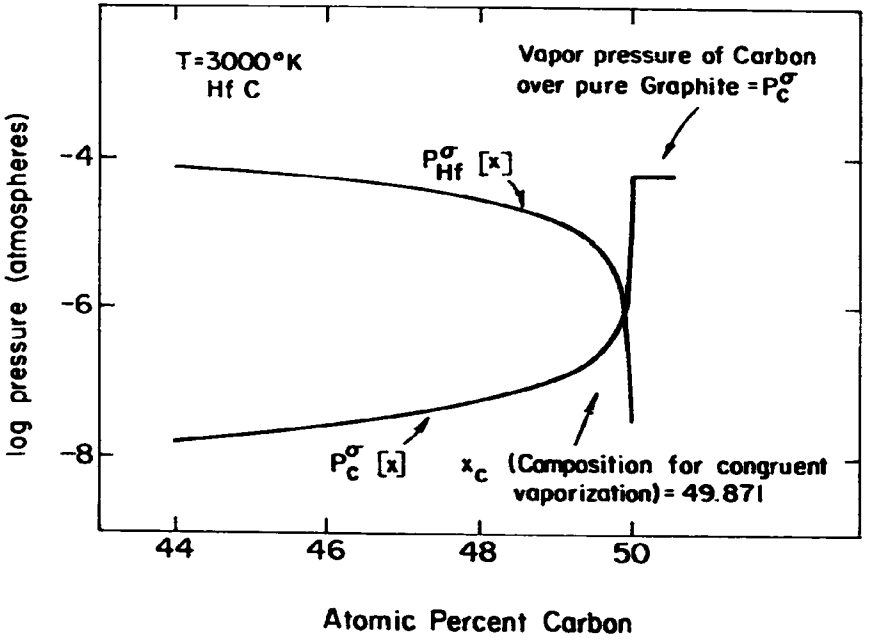

Fig. 11 -Calculated compositional dependence of the vapor pressure of Hf and C over the Hf C^σ phase at 3000°K.

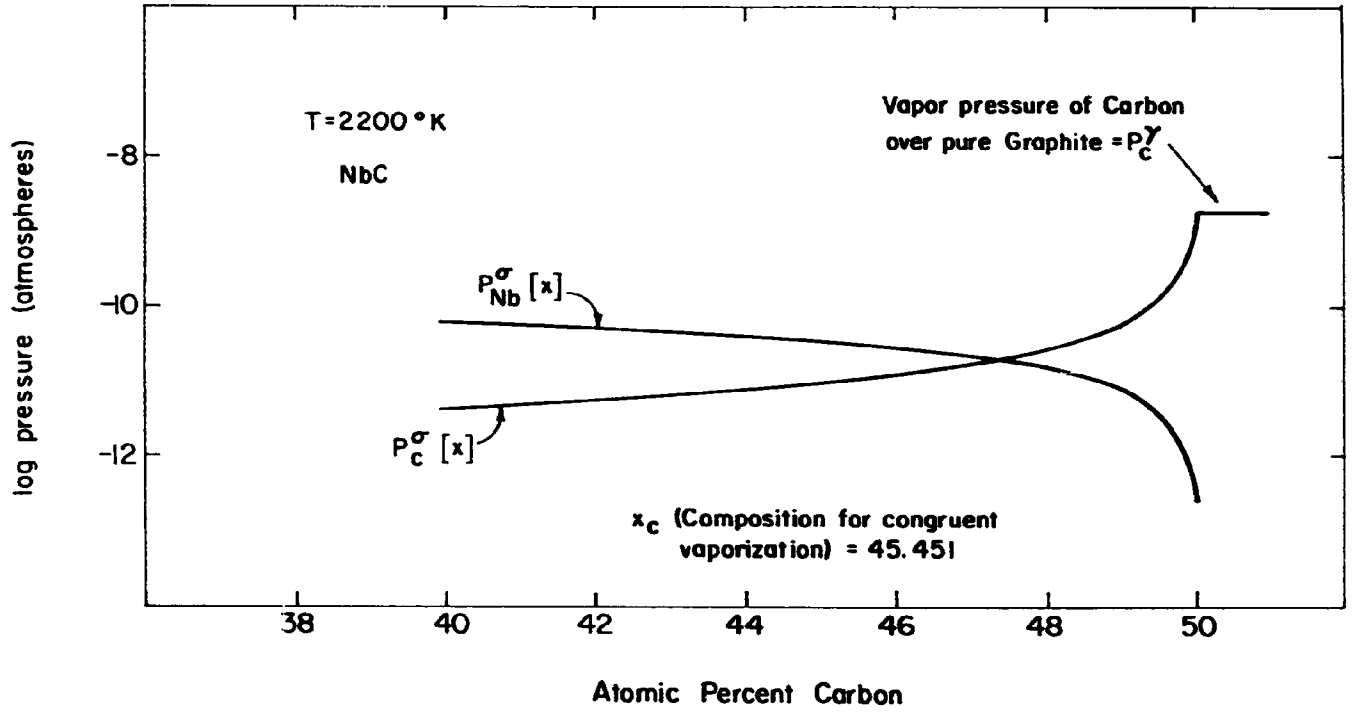

Fig. 12 - Calculated compositional dependence of the vapor pressure of Nb and C over the NbC^{σ} phase at 2200°K.

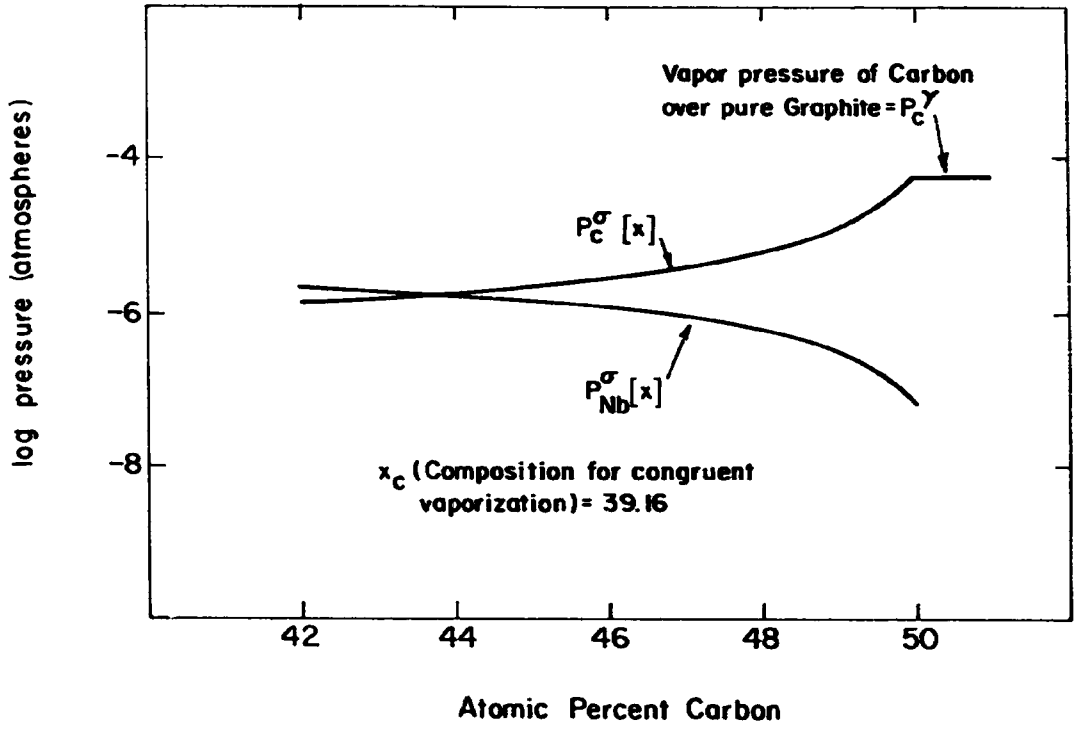

Fig. 13 - Calculated compositional dependence of the vapor pressures of Nb and C over the NbC^{σ} phase at 3000 °K.

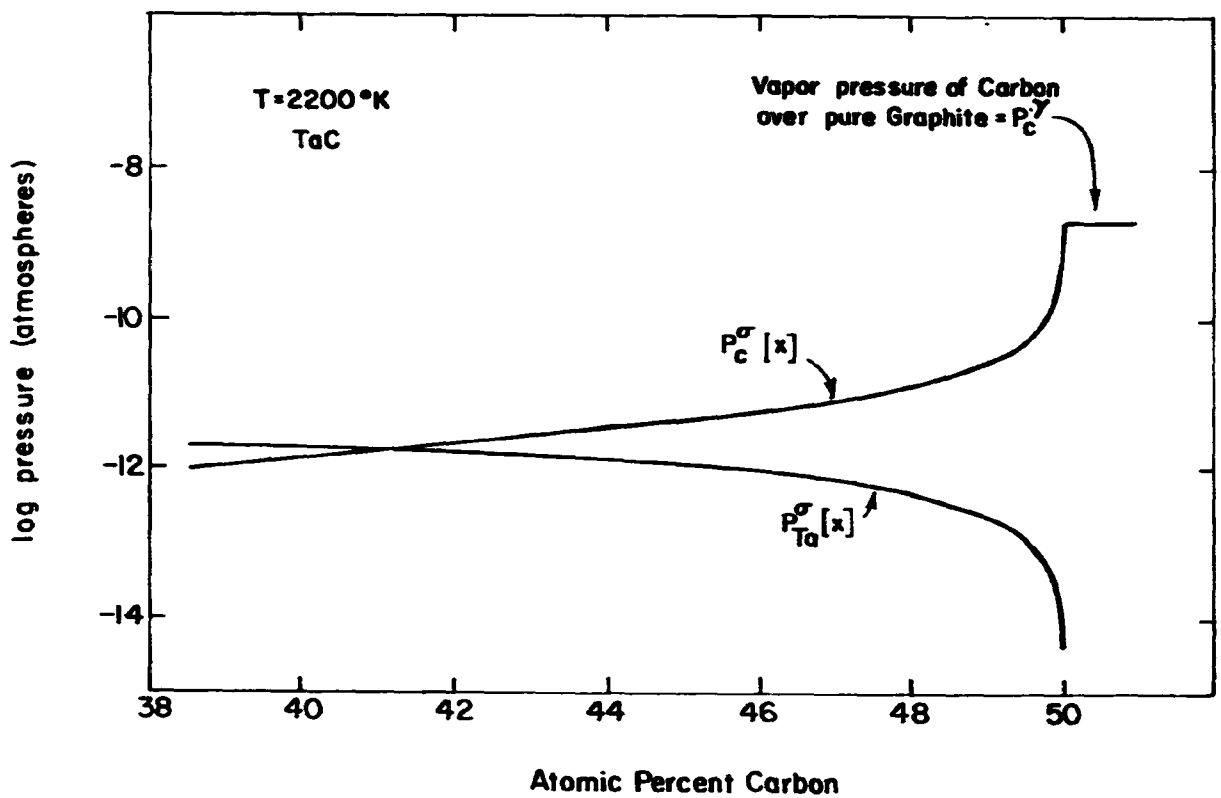

Fig. 14 - Calculated compositional dependence of the vapor pressures of Ta and C over the TaC^σ phase at 2200 °K.

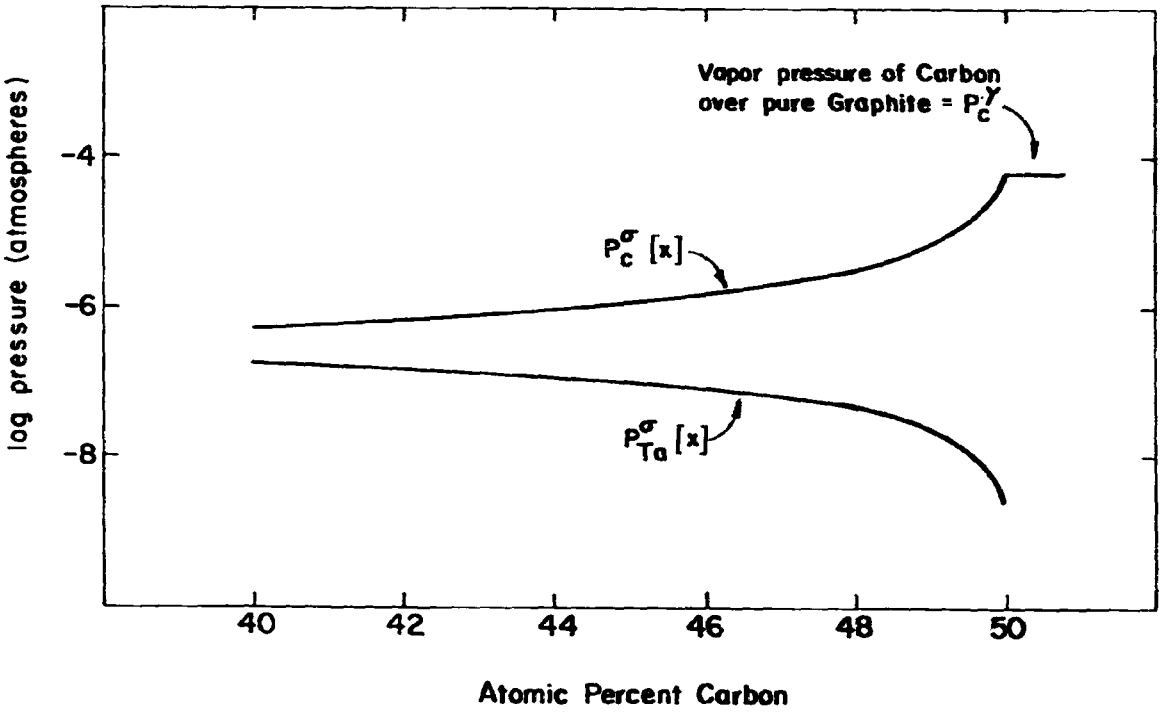

Fig. 15 - Calculated compositional dependence of the vapor pressures of Ta and C over the TaC^{σ} phase at 3000 °K.

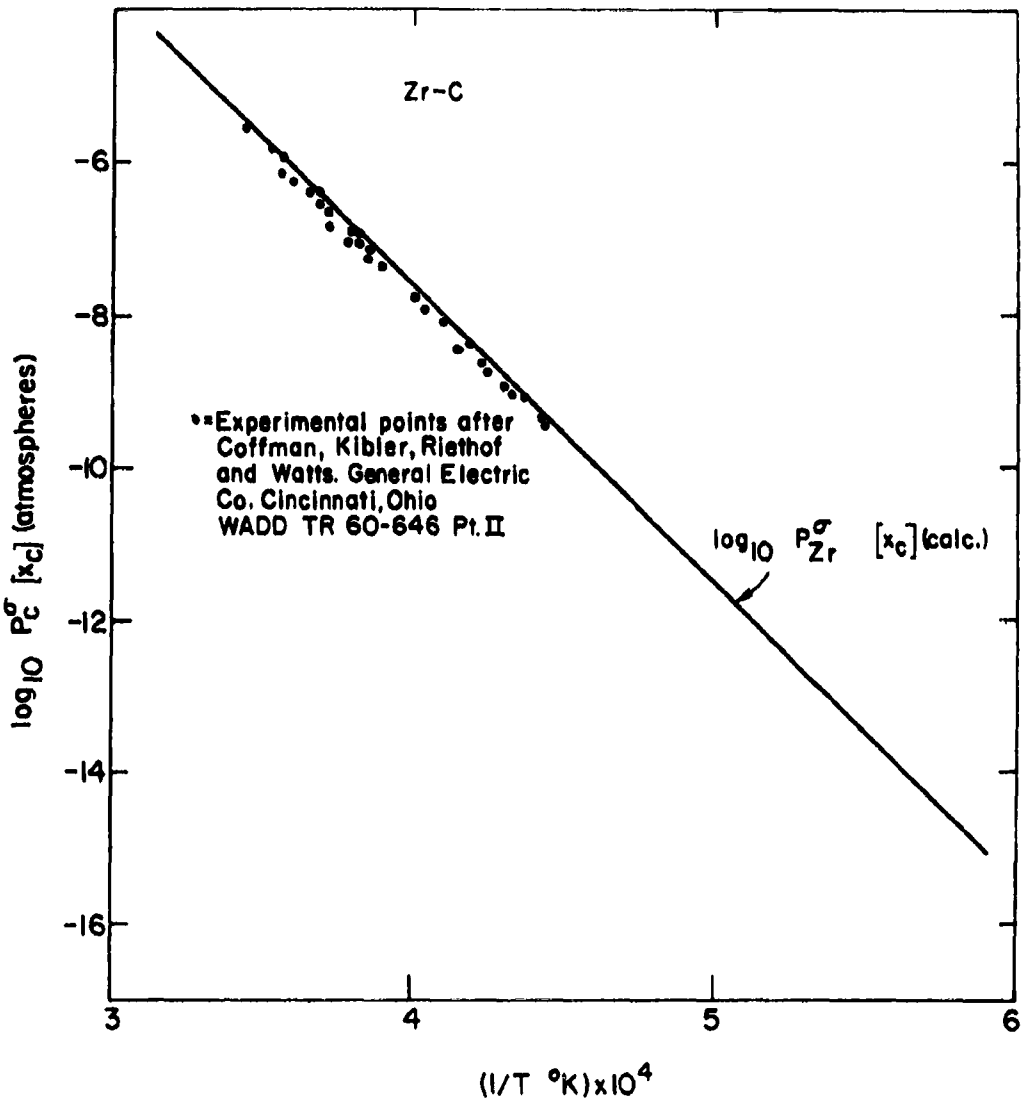

Fig. 16 - Comparison of calculated and observed vapor pressure of Zirconium over congruently vaporizing ZrC.

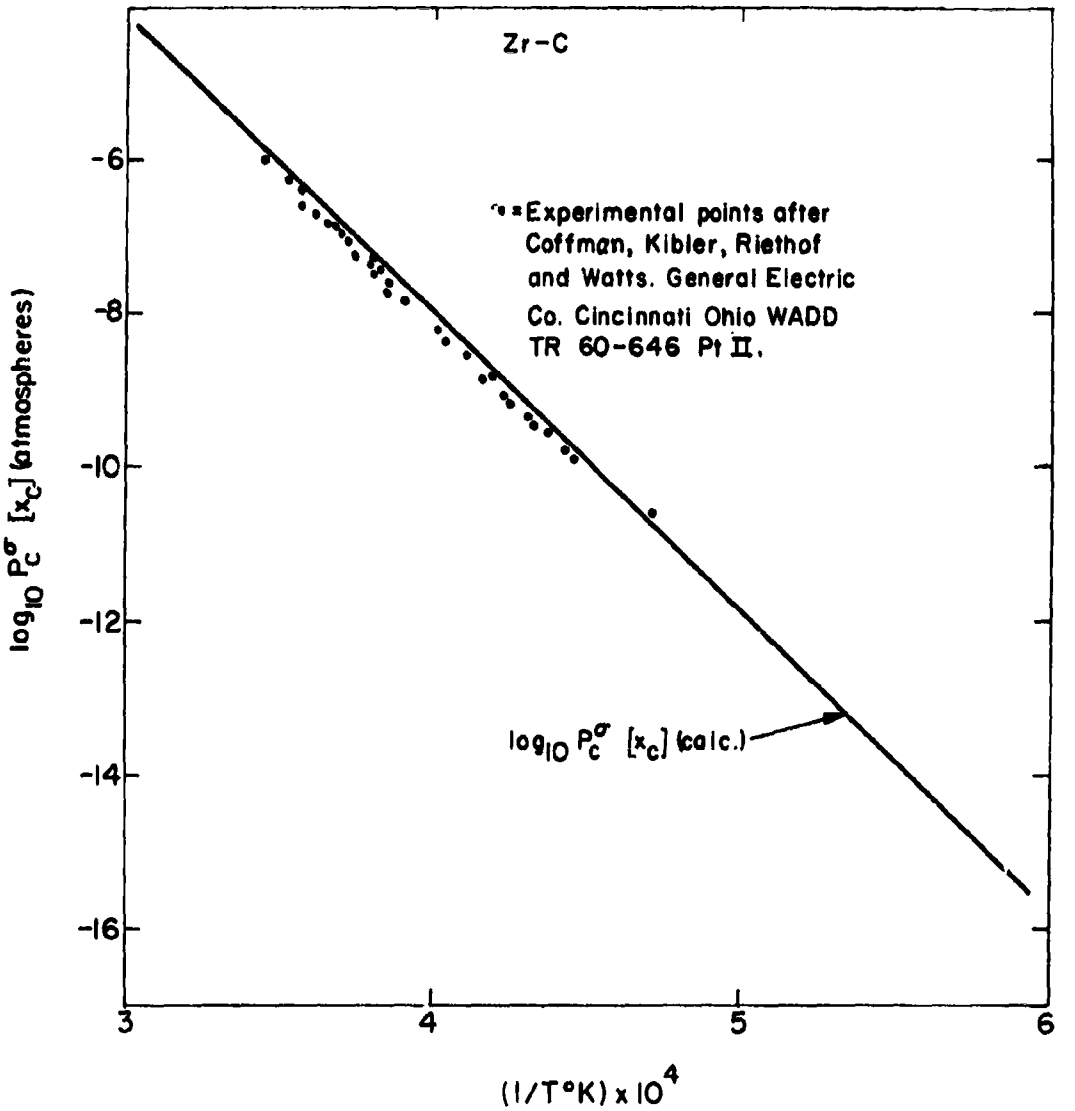

Fig. 17 - Comparison of calculated and observed vapor pressure of Carbon over congruently vaporizing Zr C.

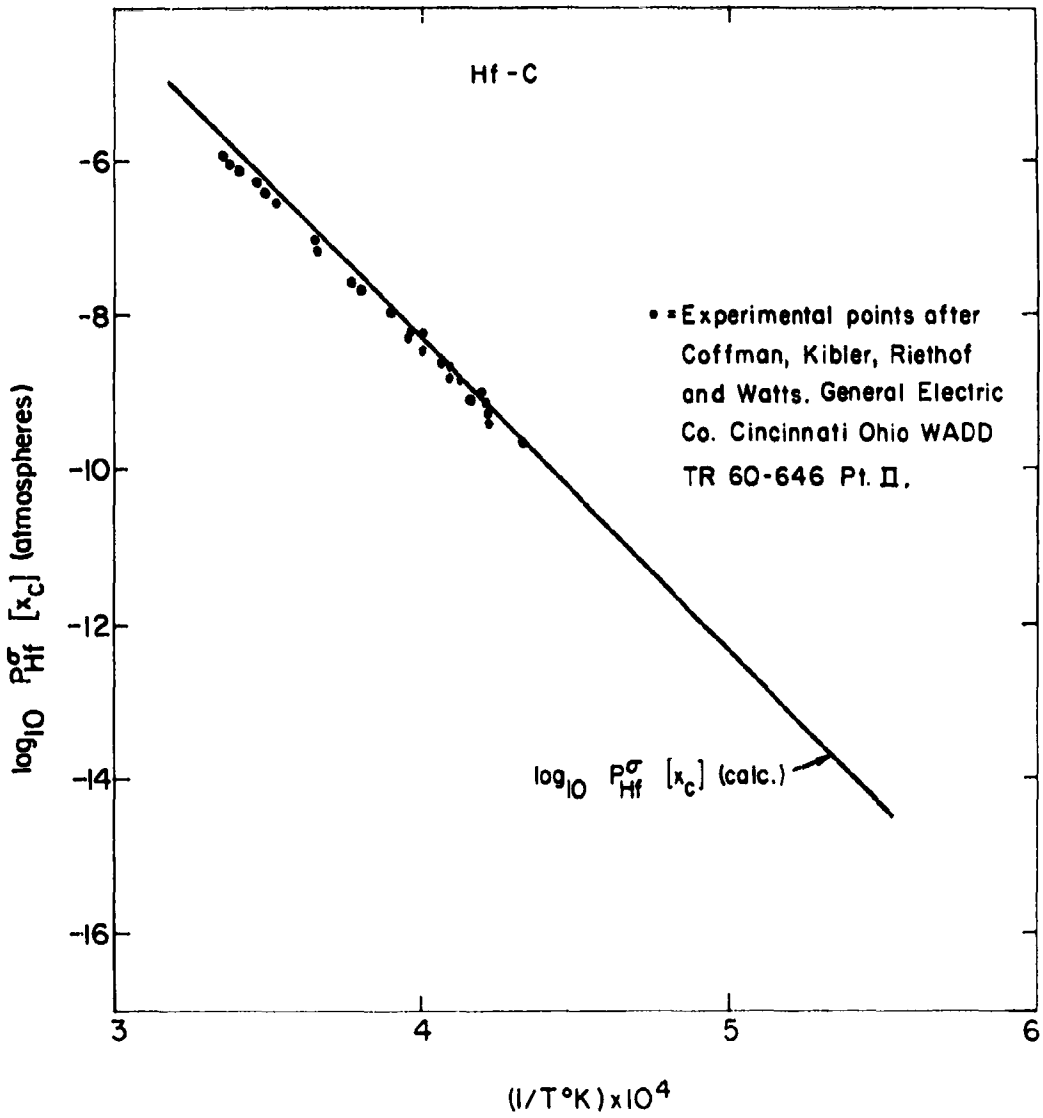

Fig. 18 - Comparison of calculated and observed vapor pressure of Hafnium over congruently vaporizing Hf-C.

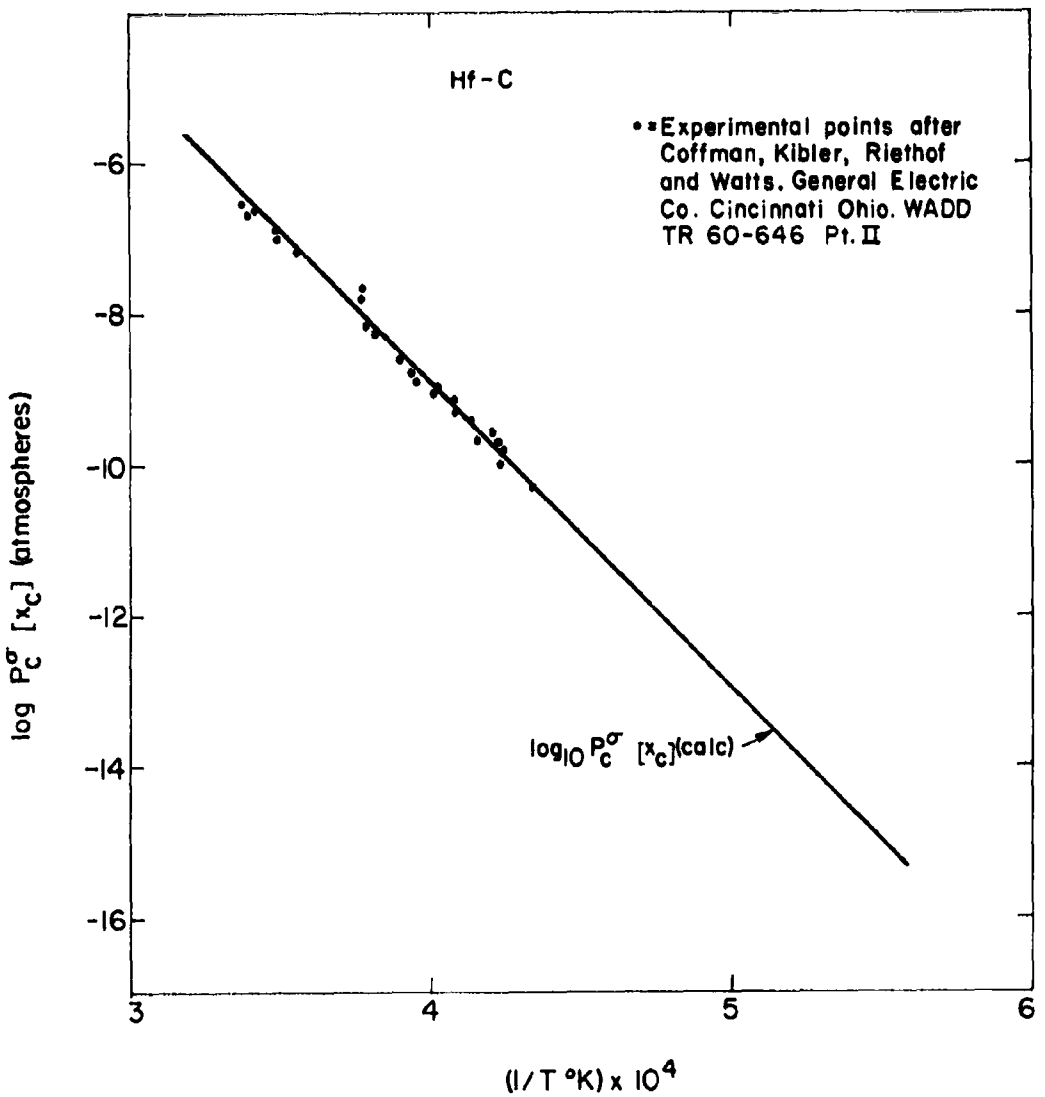

Fig. 19 - Comparison of calculated and observed vapor pressure of Carbon over congruently vaporizing Hf C.

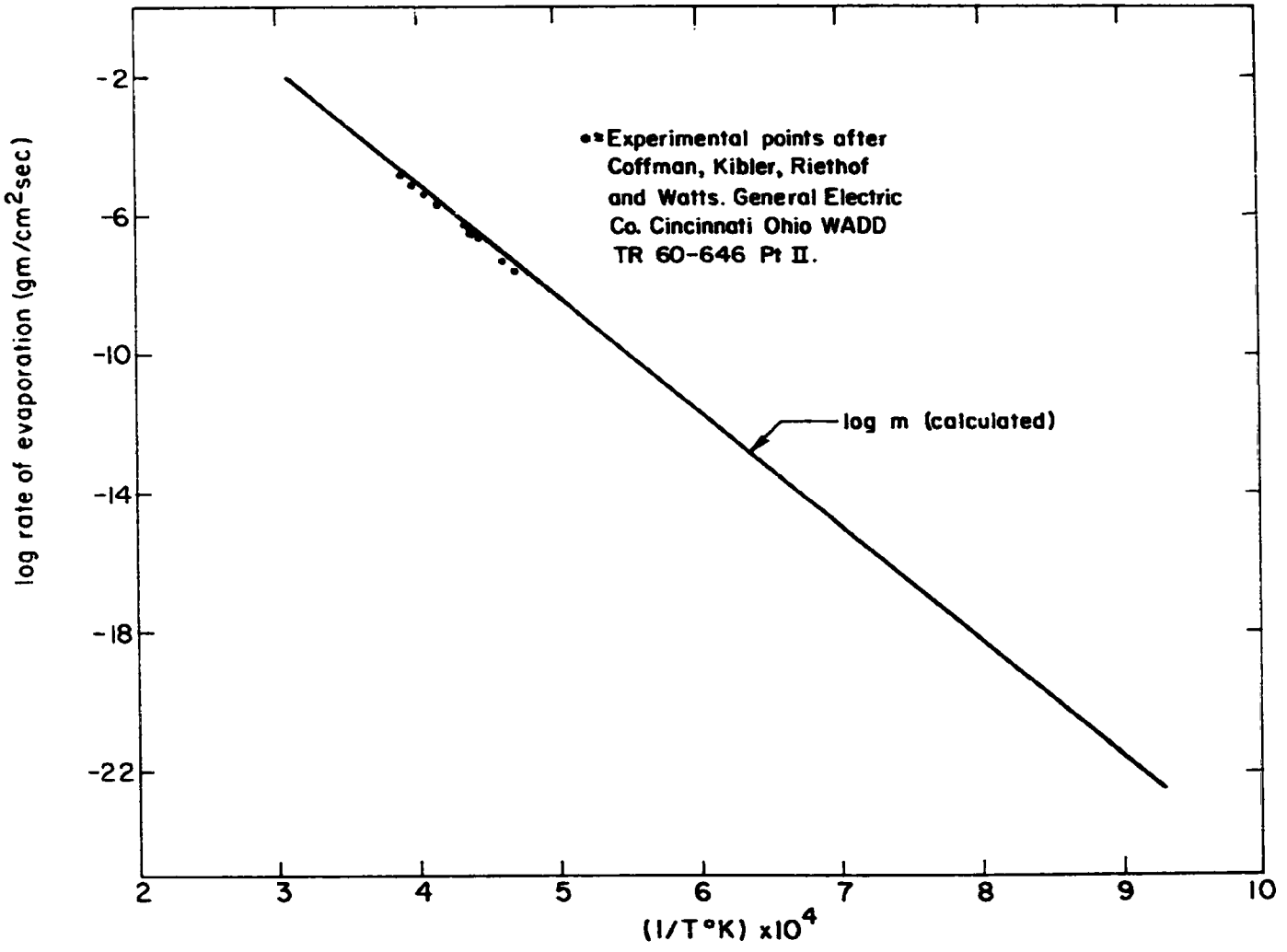

Fig. 20 - Comparison of calculated and observed rates of evaporation of Titanium Carbide.

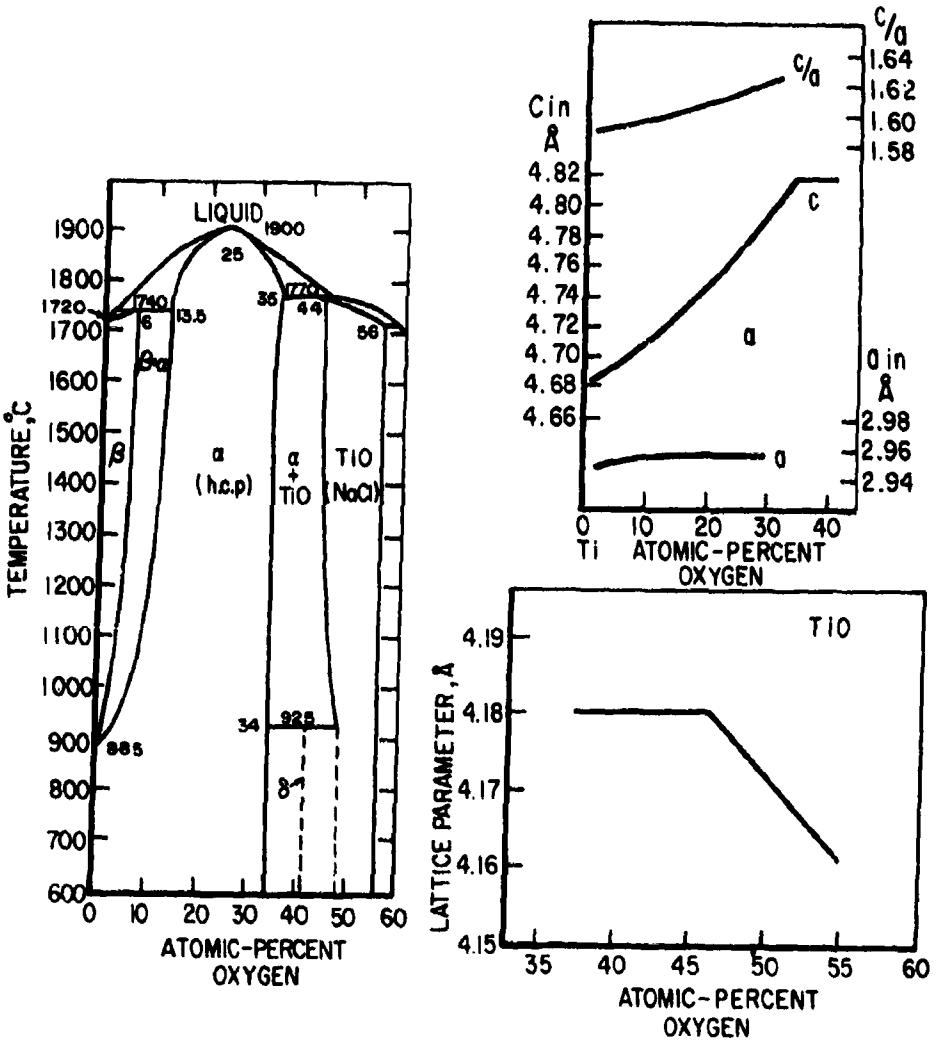

Fig.21 - Lattice parameters and phase relations in the titanium-oxygen system[22,29,33].

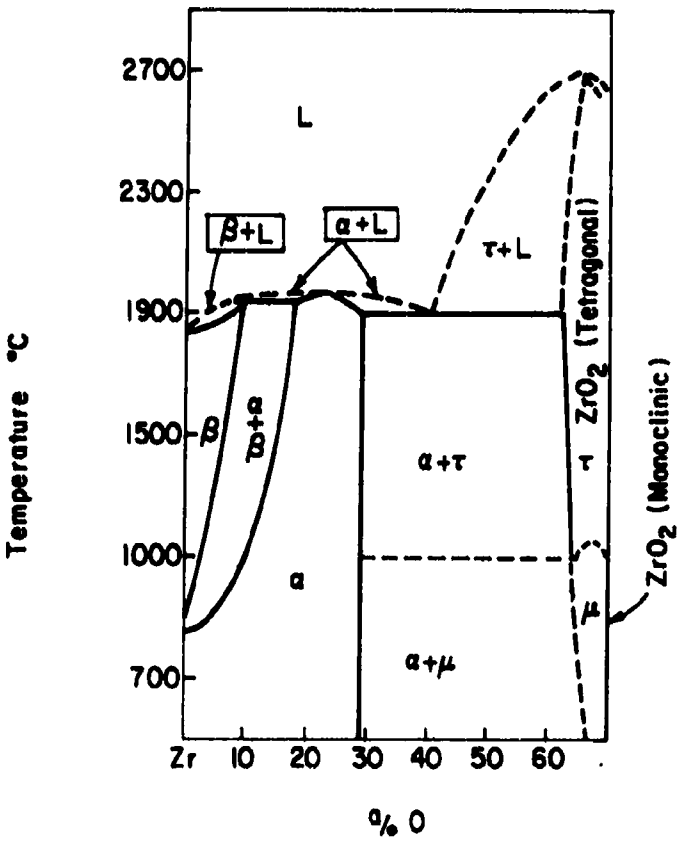

Fig.22— The Zirconium-Oxygen phase diagram (after Hansen and Anderko[22]).

between Ta and TaC is calculated on the basis that Ta_2C does not form. Recently, R. V. Sava of the Union Carbide Research Center, Parma, Ohio, performed an experiment in which a Ta-TaC couple was heated rapidly. Ta_2C did not form during the experiment and melting was observed at 2200°C (2470°K) corroborating the prediction of Fig. 5.

2.2 Discussion of the Ti-O and Zr-O Systems

Figs. 21 and 22 show the Ti-O and Zr-O phase diagrams. These differ appreciably from the Ti-C and Zr-C situations in that considerable solubility of oxygen in both the α(h. c. p.) and β(b. c. c.) forms of these metals is exhibited at one atmosphere, several "compounds" are formed (in Ti-O) and the σ structure (which appears only in the Ti-O system) does not exhibit the high temperature stability indicated in the Ti-C and Zr-C cases; moreover the most refractory compounds occur at values of x(atomic fraction oxygen) which are different from 1/2.

Since the thermodynamic properties of the Ti-O system have been most extensively evaluated[34-42], it is instructive to start with a discussion of this system. In line with the stated reference state convention, the free energy of oxygen (gaseous) at temperatures above 500°K and one atmosphere will be approximated by *Eq. (25),

$$\frac{1}{2}F^{G}_{O_2} \simeq 400 - 4.22\,T \ln T/2.74 \text{ cal/g. at.} \qquad (25)$$

Kubaschewski and Dench[33, 34] have measured the partial molar free energies of oxygen for several Ti-O alloys in the interstitial β and α range. They combined these data with published values for the free energy of formation of TiO^{σ}, Ti_2O_3, and higher oxides to draw curves for the partial molar free

*This expression differs by about 850 cal/g. at. from the usually tabulated data[26] which gives the room temperature enthalpy of a mol of oxygen as 2075 cal/mol. This value refers to an ideal gas between 0°K and 298°K. In spite of this, the

energies of titanium ($\bar{F}^{\alpha}_{Ti}[x] - F^{\beta}_{Ti}$) and oxygen ($\bar{F}^{\alpha}_{O}[x] - 1/2\ F^{G}_{O_2}$) at 1273°K. These curves are naturally consistent with the tabulated values for the other compounds. Mah, Kelley and co-workers[36] measured the enthalpy of formation of α Ti-O alloys at 298°K for $x \leq 0.25$ while Ariya, Morozova, and Volf[37] did similar measurements over the range $0.20 \leq x \leq 0.70$. Mah et al[36] also measured the specific heat of two alloys containing 0.058 and 0.25 atomic fractions of oxygen. Hepworth and Schuhmann[38] measured the pressure of hydrogen over Ti-O-H alloys from which they deduced the activity of oxygen in Ti-O alloys at 1073°K over the range $0 \leq x \leq 0.14$. These calculations were made on the basis of an infinitely dilute standard state and then converted to absolute activities by using the data of Mah et al[36].

Veinbachs, Silver and Komarek[39] measured the activity of oxygen in the Ti-O system over the temperature range $1100°K < T < 1300°K$ for alloys containing up to 25 a/o oxygen. They used their data to compute partial entropies and enthalpies for oxygen. The enthalpy data yielded heat of solution in the dilute solution range which agree with the calorimetric values of Mah et al. In this range, the activity data agreed with those of Kubaschewski[34, 35] and Hepworth[38]. However, at higher compositions the results of Veinbachs et al[39] differ from those deduced by Kubaschewski. Consequently these data do not agree well with the published data for titanium compounds.

---

tables give the 298°K entropy (49.00 cal/mol) based on solid oxygen at 0°K. The enthalpy at 298°K based on solid oxygen at 0°K is nearer[43] 3750 cal/mol which is the value used in the present convention. The difference between 3750 and 2075 (divided by 2 i.e. per gm. atom) accounts for the abovementioned difference.

On the basis of their entropy data, Veinbachs et al[39] were able to show that the positional entropy of α Ti-O alloys was consistent with an ideal interstitial solid solution (i.e. Eq. A2-7, n =1 since α is h.c.p. and z = 1).

Eqs. (A2-1-8) indicate that the thermodynamic properties of an interstitial solid solution can be specified if several parameters are known*. Thus, H^{α}_{TiO}, A, and $\theta^{\alpha}_{Ti}[x]$ need to be specified. The latter function can be estimated from a knowledge of the atomic volumes, the melting points, and the atomic weights of Ti and O (Fig. 6). In this estimation procedure, T^{α}_{Ti} is taken[1] as 1730°K. The resultant $\theta^{\alpha}_{Ti}[x]$ curve is approximately

$$\theta^{\alpha}_{Ti}[x] \sim 365\ (1-x)(1+2x) \qquad (26)$$

This equation can be used (with A2-2) to estimate the specific heat and entropy on the basis of the two-Debye θ method[5] ignoring contributions of the electronic specific heat**. Comparison of the calculations with the reported specific heat data $50^{\circ}K \leq T \leq 300^{\circ}K$[36] is within 3% for x = 0.058 and 10% for x = 0.25. The room temperature entropy values for x = 0.058 are 6.78 cal/g.at. °K (observed) and 6.6 (calculated) while for x = 0.25, 5.15 is observed and 5.50 is calculated. Although Mah et al[36] suggest that the excess vibrational entropy is zero (i.e. the partial vibrational entropies of Ti and O are independent of composition) the abovementioned estimation procedure yields concentration dependent partials. This arises from the pronounced maximum in the melting point at x = 0.25. It would be of interest to have measurements of the specific

---

*Both z and n are unity as indicated above.

**Low temperature specific heat measurements[40] on α Ti-O alloys (1-4°K) show the electronic specific heat to be small.

heat (50-300°K) at a higher oxygen content within the α field ($0.25 \leq x \leq 0.33$) in order to resolve this point.

The remaining parameters $H^{\alpha}_{TiO}[0^{\circ}K]$ and A can be directly evaluated from Kubashewski's values for the compositional dependence of $(\overline{F}^{\alpha}_{O} - 1/2F^{G}_{O_2})$ at 1273°K. The results, A = -24,650 and $H^{\alpha}_{TiO}[0^{\circ}K]$ = -60,000 cal/g.at. reproduce the published results to within 1%. The latter parameter leads to an enthalpy of formation which closely approximates the value suggested[26] for the stable form of TiO. This is not surprising in view of the structural similarity between the δ structure and a h.c.p. metal lattice in which all of the interstitial sites are filled. Moreover, extrapolation of the α lattice parameters (Fig. 6) to x = 0.5 leads to a volume of 5.6 cm^3/g.at. vs 5.5 cm^3/g.at. for the δ structure. On this basis (ref. 20, Fig. 93) one would expect very similar heats of formation. Finally substitution of these parameters into Eq. (A2-8) permits calculation of the enthalpy of formation of α Ti-O alloys which agree to within 3% (or better) with the values measured by Mah et al[33]. The final representation of the Ti and O partials are given by Eqs. (27) and (28),

$$\overline{F}^{\alpha}_{Ti} - F^{\alpha}_{Ti} = RT \ln (1-2x)(1-x)^{-1} - 49,300x^2 + 3RT(\ln(1+2x)(1-x) - x(1-4x)(1-x)^{-1}(1+2x)^{-1}) \quad (27)$$

and

$$\overline{F}^{\alpha}_{O} - 1/2\, F^{G}_{O_2} = -1/2F^{G}_{O_2} - 120,000 + 3RT \ln 632/T + RT \ln x(1-2x)^{-1} - 24,650(1-4x+2x^2) + 3RT(\ln(1+2x)(1-x) + (1-4x)(1+2x)^{-1}) \quad (28)$$

As a final check on Eq. (27), this equation can be used to calculate $x_{\alpha\beta}$ vs. T for comparison with Fig. 6. This calculation is performed by

equilibrating the partials of Ti across the $\alpha + \beta$ field and applying Eq. A2-6 to the β phase (n=3) for dilute solutions. The $\Delta F_{Ti}^{\alpha \rightarrow \beta}[T]$ values used for this calculation were taken from reference (1). The agreement between the calculated $x_{\alpha\beta}$ vs. T curve agrees to within 2 a/o with the observed curve Fig. (6) for $1300^{\circ}K \leq T \leq 2000^{\circ}K$.

Turning to the TiO σ phase, we make the first approximation (as in the case of TiC, ZrC, and TaC) that α is very small. Consequently Eqs. (A1-11-14) can be applied. Designating the Ti_2O_3 phase by the symbol λ, the following relations can be written at $1273^{\circ}K$.

$$\overline{F}_{Ti}^{\alpha}\Big|_{x_{\alpha\sigma}} = \overline{F}_{Ti}^{\sigma}\Big|_{x_{\sigma\alpha}} - \overline{F}_{Ti}^{\beta} - F_{Ti+} + RT \ln(1-2x_{\sigma\alpha})/4\alpha^2(1-x_{\sigma\alpha}) \qquad (29)$$

$$\overline{F}_{O}^{\alpha}\Big|_{x_{\alpha\sigma}} = \overline{F}_{O}^{\sigma}\Big|_{x_{\sigma\alpha}} - 1/2\, F_{O_2}^{G} - F_{O+} + RT \ln x_{\sigma\alpha}/(1-2x_{\sigma\alpha}) \qquad (30)$$

where $x_{\alpha\sigma} = 0.337$ and $x_{\sigma\alpha} = 0.465$ from Fig. 6, and

$$\overline{F}_{Ti}^{\lambda}\Big|_{x_{\lambda\sigma}} = \overline{F}_{Ti}^{\sigma}\Big|_{x_{\sigma\lambda}} - F_{Ti}^{\beta} - E_{Ti+} + RT \ln(1-x_{\sigma\lambda})/(2x_{\sigma\lambda}-1) \qquad (31)$$

$$\overline{F}_{O}^{\lambda}\Big|_{x_{\lambda\sigma}} = \overline{F}_{O}^{\sigma}\Big|_{x_{\sigma\lambda}} - 1/2\, F_{O_2}^{G} - F_{O+} + RT \ln(2x_{\sigma\lambda}-1)/4\alpha^2 x_{\sigma\lambda} \qquad (32)$$

where $x_{\sigma\lambda} \sim 0.56$ and $x_{\lambda\sigma}$ is near 0.6.

In these equations $\overline{F}_{Ti}^{\alpha}$ and $\overline{F}_{O}^{\alpha}$ are given by Eqs. 27 and 28 while F_{Ti+}, F_{O+} and α are the free energies of formation of titanium and oxygen vacancies and the vacancy parameter for the Ti-O σ phase at $1273^{\circ}K$. Since $\overline{F}_{O}^{\alpha}[0.337] - \frac{1}{2} F_{O_2}^{G} = -90,500$ cal/g.at. at $1273^{\circ}K$ from Eq. (28), Eq. 30 yields

$$F_{O+} \simeq +95,300 \text{ cal/g.at.} \qquad (33)$$

Multiplication of Eq. 31 by 0.4 and Eq. 32 by 0.6 and addition yields

$$\Delta F^{\lambda}\,[0.6,\ 1273] \approx 0.8\,\Delta F^{\sigma}[0.5,\ 1273] - 0.2F_{O+} - 0.4\,RT\ln 2\alpha$$
$$+ 0.2\,RT\ln(2x_{\sigma\lambda} - 1)(1 - x_{\sigma\lambda})^{2}\,x_{\sigma\lambda}^{-3} \qquad (34)$$

Where ΔF^{λ} and ΔF^{σ} are the free energies of formation of the "Ti_2O_3" and "TiO" stoichiometric phases (cal/g.at.). Substitution of the proper numerical values[26] yields

$$RT\ln 2\alpha \sim -6500 \text{ cal/g.at.} \quad \text{or} \quad \alpha \sim 0.05 \qquad (35)$$

Thus α is not small and the approximations introduced by Eqs. 29-32 are not valid. These equations are now rewritten using the more accurate expressions in Table A1-1 and applied over the range $1273^{\circ}K \leq T \leq 2000^{\circ}K$ to solve for α, F_{Ti+} and F_{O+} (since we can write four equations at each temperature). This procedure yields the following results for the TiO^{σ} phase

$$F_{Ti+} \sim 18{,}100 - 3.3\,T \text{ cal/g.at.} \qquad (36)$$

$$F_{O+} \sim 119{,}800 - 19.9T \text{ cal/g.at.} \qquad (37)$$

$$RT\ln\alpha/(1-2\alpha) \sim -8200 \text{ cal/g.at.} \qquad (38)$$

On the basis of these results, we can approximate the enthalpy of formation of Ti and O vacancies as $H_{Ti+} \sim 18.1$ kcal/g.at. and $H_{O+} \sim 119.8$ kcal/g.at. Substitution of these results into Eqs. (A1-25-26) permits calculation of the compositional dependence of the enthalpy of formation of TiO^{σ} for comparison with the results of Ariya et al[37]. Comparison of the calculated and observed values shown in Table I is satisfactory.

As noted previously, the value for the vacancy parameter α for the TiO^{σ} is surprisingly large (Eqs., 35, 38). However, this is quite consistent

TABLE I

COMPARISON OF THE CALCULATED AND OBSERVED[37] COMPOSITIONAL DEPENDENCE OF THE ENTHALPY OF FORMATION OF TiO^{0}

x at. fr. oxygen	$-\Delta H^{\sigma}[298]$ kcal/g.at. obs.[37]	calc.	x at. fr. oxygen	$-\Delta H^{\sigma}[298]$ kcal/g.at. obs.[37]	calc.
0.447	57.29±0.14	56.8	0.502	62.88±0.02	63.0
0.466	60.18±0.12	59.0	0.506	63.42±0.02	63.3
0.484	61.40±0.05	61.0	0.528	65.43±0.02	65.3
0.492	62.26±0.03	61.9	0.548	67.34±0.04	67.1
			0.556	68.43±0.03	67.8
0.500	(Interpolated) 62.80	62.8	0.560	68.86±0.02	68.4

TABLE II

COMPARISON OF CALCULATED AND OBSERVED[41, 42] VACANCY CONCENTRATIONS IN THE TiO^{0} PHASE

x at. fr. oxygen	Percentage of Vacant Ti Sites obs.[41, 42]	calc. (α=0.079)	Percentage of Vacant O Sites obs.[41, 42]	calc. (α=0.079)
0.41	4	7.0	34	35.2
0.50	15	15.8	15	15.8
0.53	19	21.4	9	11.4
0.56	23	28.2	4	8.8
0.57	26	30.6	2	8.0

CALCULATED TEMPERATURE DEPENDENCE OF α (Eq. 38)

$T^{\circ}K$	1273	1400	1600	1800	2000
α	0.036	0.047	0.066	0.084	0.101

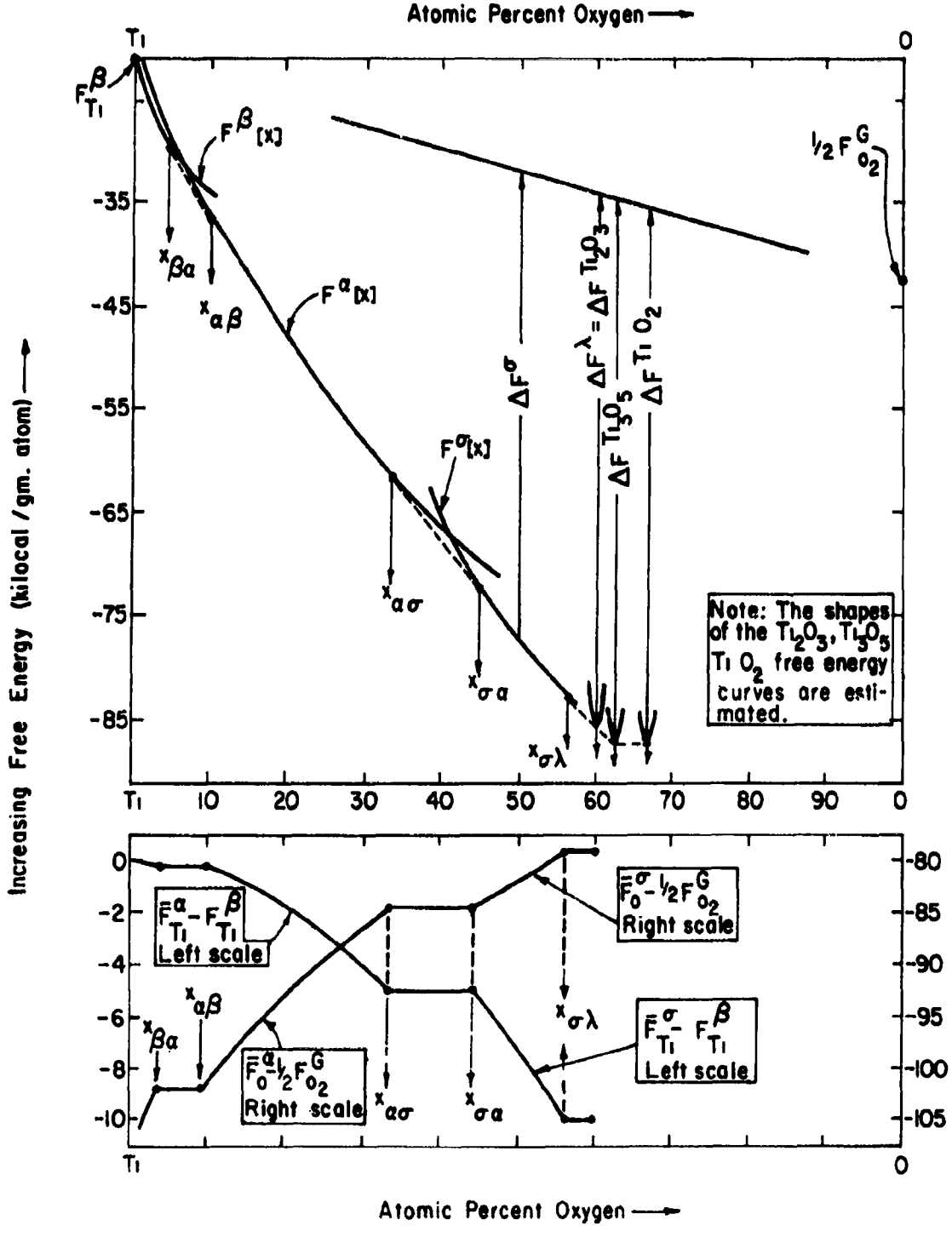

Fig. 23 - Calculated integral and partial free energies in the Ti-O system at 1600°K

with the results of Ehrlich[41, 42]. Ehrlich determined the fraction of vacant Ti and O sites by performing lattice parameter and density measurements on a series of TiO^{σ} alloys quenched from high temperatures. His results, along with calculated vacancy concentrations (Eqs., 38, A1-1-3, and Table A1-I) corresponding to 1500°C ($\alpha = 0.079$) are given in Table II. The agreement is quite good.

This comparison is particularly satisfying since it offers support for the physical basis of the model since the calculation of α is performed on thermodynamic grounds and yields values of α which compare quite favorably with those derived from physical measurements.

As a final illustration of the properties of the TiO^{σ} phase it is instructive to plot the integral and partial free energies at 1600°K as a function of composition using Eqs. (27), (28), (36-38), and the equations in Table A1-I. Values for the free energy of formation used throughout are those tabulated by Gleiser and Elliot[26].

It is interesting to compare Figs. 3 and 4 for ZrC^{σ} with Fig. 23 for TiO^{σ} in order to examine the effects of the parameter α and the free energies of formation of metal and nonmetal vacancies on the shape of the F^{σ}-x curve. Examination of these figures shows that a smaller value of α (i.e. 10^{-5} for ZrC vs 10^{-1} for TiO) leads to a "sharper" F^{σ}-x curve and a larger variation in partial free energies across the single phase field. Moreover when the free energy of formation of vacancies of one of the species is small relative to the free energy of formation at stoichiometry (i.e. Ti in TiO) the F^{σ}-x curve loses its characteristic minimum.

The Zr-O system (Fig. 22)is very similar to Ti-O system. The chief differences are the slightly lower values for the compositional limit of the

α phase, the higher melting point of ZrO_2 (relative to TiO_2) and the absence of stable compounds between the α phase and ZrO_2^T and ZrO_2^M (we will use these phase designations for the tetragonal and monoclinic forms of ZrO_2). There have been references[44,29] to a metastable ZrO^σ. All of these observations are interrelated and stem from the greater stability of ZrO_2 relative to TiO_2. If the tabulated free energy of formation of ZrO_2 were used in place of that for TiO_2 in construction of Fig. 23, then the x = 0.667 minimum would permit a common tangent to be drawn between the T and α phase below the σ, Ti_2O_3 and Ti_3O_5 phase thus leading to phase relations similar to those shown in Fig. 22.

Veinbachs et al[39] and Kubachewski and Dench[45] have measured the activity of oxygen in the α Zr-O phase. Veinbachs et al suggested that the positional entropy of α Zr-O alloys is ideal. Using this information and the procedure described earlier to estimate the properties of the interstitial Ti-O α solid solutions yield the following results:

$$\theta^{\alpha}_{Zr}[x] = \theta^{\alpha\alpha}_{Zr} \simeq 260^{\circ}K^{(1)},\ \theta^{\alpha}_{O}[x] = 621^{\circ}K$$

$$A = -23,800 \text{ cal/g.at. and } H^{\alpha}_{ZrO}[0^{\circ}K] = -63,000 \text{ cal/g.at.}$$

Comparison of these values with the Ti-O parameters discussed earlier shows the similarity between these systems. The analogues of Eqs. (27) and (28) for the Zr-O system are,

$$\bar{F}^{\alpha}_{Zr} - F^{\alpha}_{Zr} = RT \ln(1-2x)(1-x)^{-1} - 47,600x^2 \text{ cal/g.at.} \quad (39)$$

$$\bar{F}^{\alpha}_{O} - 1/2F^{G}_{O_2} = -1/2\, F^{G}_{O_2} - 126,000 + 3\, RT \ln 621/T$$

$$+ RT \ln x(1-2x)^{-1} - 23,800(1-4x+2x^2) \text{ cal/g.at.} \quad (40)$$

These equations can be used to calculate $\overline{F}^{\alpha}_{Zr} - F^{\beta}_{Zr}$ by using the tabulated $\Delta F^{\alpha\rightarrow\beta}_{Zr}[T]$ values[1]. As was the case for the Ti-O system, the $x_{\alpha\beta}$ vs T curve is calculated in agreement with the published $x_{\alpha\beta}$ vs T curve (Fig. 7). Equilibrating the partials of Zr and O across the $\alpha + T$ fields yields equations analogous to Eqs. (29) and (30). Assuming α (the vacancy parameter), for ZrO_2 is small yields ($1300^{\circ}K \leq T \leq 2173^{\circ}K$)

$$\overline{F}^{\alpha}_{Zr}\Big|_{x_{\alpha T}} = \overline{F}^{T}_{Zr}\Big|_{x_{T\alpha}} \approx F^{\beta}_{Zr} - F_{Zr+} + RT \ln(2-3x_{T\alpha})^2/27\alpha^3(1-x_{T\alpha})^2 \qquad (41)$$

$$\overline{F}^{\alpha}_{O}\Big|_{x_{\alpha T}} = \overline{F}^{T}_{O}\Big|_{x_{T\alpha}} \approx 1/2\, F^{G}_{O_2} - F_{O+} + RT \ln x_{T\alpha}/2-3x_{T\alpha} \qquad (42)$$

$$\text{where } 3\Delta F^{T} \approx - F_{Zr+} - 2F_{O+} - 3RT \ln 3\alpha/4^{1/3} \qquad (43)$$

In these equations, ΔF^{T} is the free energy of formation of stoichiometric ZrO_2^{T}, F_{Zr+} and F_{O+} are the free energies of formation of Zr and O vacancies in ZrO_2^{T}, and $3\alpha/4^{1/3}$ is the fraction of vacant sites in the T phase at x = 2/3.

Eq. (41) can be solved for $F_{O+}[T]$ by using Eq. 40 and the phase diagram yielding:

$$F_{O+} \approx 128,400 - 17.5T \qquad (44)$$

Eqs. (39) and (41) can be used together with the phase diagram to solve for the sum of $F_{Zr+} + 3RT\ln\alpha$ and the result checks with Eq. (43).

$$F_{Zr+} + 3RT\ln\alpha = +3000 - 12.2T \qquad (45)$$

If the solubility of oxygen in ZrO_2 (i.e. the high oxygen phase boundary of the ZrO_2 phase) were known, then α (and F_{Zr+}) could be estimated explicitly. Ackerman, Thorn and Winslow[46] have measured the vapor pressure of various gaseous species over ZrO_2 at $2750^{\circ}K$. They suggest a value of α near

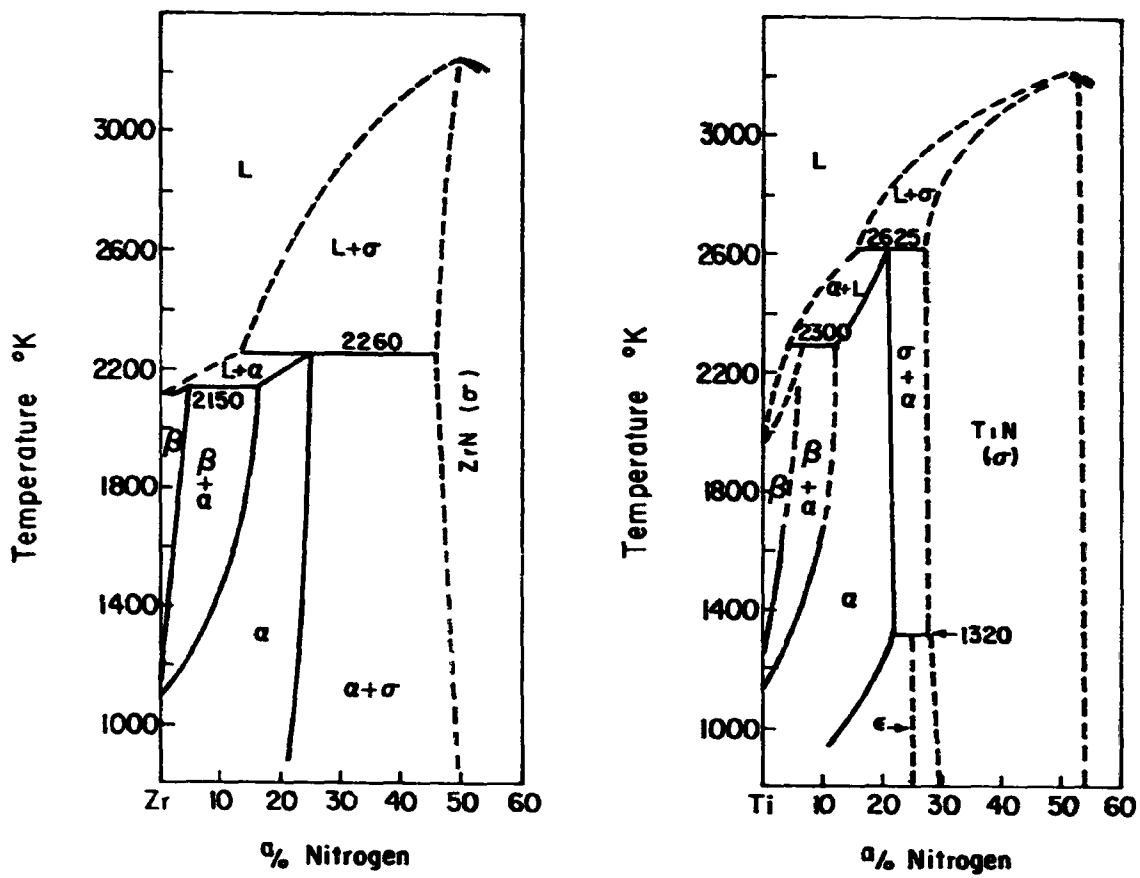

Fig. 24 – The Zirconium–Nitrogen and Titanium–Nitrogen phase diagrams (after Hansen and Anderko[22]).

10^{-3} at this temperature. Hence $3RT\ln\alpha \simeq -113,100$ cal/g.at. and $F_{Zr+} \simeq 116,100 - 12.2T$. This result implies that for ZrO_2 the free energies of vacancy formation of both species are of similar magnitudes.

2.3 Discussion of the Ti-N and Zr-N Systems

The titanium-nitrogen and Zr-N systems are quite similar to each other and to the Ti-O and Zr-O systems in some respects. Fig. 24 shows the established phase diagrams which indicate stabilization of the α interstitial solid solutions and refractory δ phases. Since there do not appear to have been any complete studies of the thermodynamic properties of the α solutions, the thermodynamic properties will be estimated in a manner similar to the procedure used for the Ti-O and Zr-O α solutions. In the case of Ti-N we find that the compositional dependence of the Debye temperatures is given by Eq. (46).

$$\theta^{\alpha}_{Ti}[x] \simeq 365\ (1+x),\ \theta^{\alpha}_{N}[x] \simeq 675\ (1+x) \tag{46}$$

The values of A and $H^{\alpha}_{TiN}[0^{\circ}K]$ are found to be -18,600 and -39,000 cal/g.at. respectively, thus the partial free energies of Ti and N are approximately (i.e. Eqs. A2-6-7)

$$\bar{F}^{\alpha}_{Ti} - F^{\alpha}_{Ti} = RT\ln(1-2x)(1-x)^{-1} - 37,200x^2 + 3RT\,(\ln(1+x) - x(1+x)^{-1}) \tag{47}$$

and*

$$\bar{F}^{\alpha}_{N} - 1/2F^{G}_{N_2} = -1/2F^{G}_{N_2} - 78,000 + 3RT\ln 675/T + RT\ln x(1-2x)^{-1}$$

$$-18,600\,(1-4x+2x^2) + 3RT\,(\ln(1+x) + (1-x)(1+x)^{-1}) \tag{48}$$

As in the case of Ti-O and Zr-O, Eq. (47) can be used to calculate the $x_{\alpha\beta}$ vs T curve for comparison with Fig. 24. The differences are less than

---

*As in the case of oxygen (see section 2.2) the values used above are slightly different from the tabulated values[26] due to the choice of standard states. This difference is +(3300-2072)/2=614 cal/g.at.

2 a/o nitrogen. Assuming the α for the TiN^{σ} phase is small and equilibrating the partials of Ti and N across the $\alpha + \sigma$ field (i.e. see Eqs. 29, 30) yields

$$F_{N+} = 82,200 - 23.3T \tag{49}$$

$$F_{Ti+} + 2RT \ln 2\alpha = -3800 + 1.75T \tag{50}$$

At the high nitrogen boundary of the σ field, $x_{\sigma N}$, $\bar{F}_N^{\sigma} = 1/2F_{N_2}^G$ hence (A1-14)

$$F_{N+} = -2RT \ln 2\alpha + RT \ln (2x_{\sigma N}-1)/(1-x_{\sigma N}) \tag{51}$$

Eqs. (49) and (51) yield

$$RT \ln \alpha = -24,700 \tag{52}$$

and

$$F_{Ti+} = 45,600 - 1.0T \tag{53}$$

The Zr-N system can be treated in a similar fashion yielding $\theta_{Zr}^{\alpha}[x] \sim 265$, $\theta_N^{\alpha}[x] \sim 665$, $A \simeq 0$ and $H_{ZrN}^{\alpha}[0] \sim -42,000$ cal/g.at. thus,

$$\bar{F}_{Zr}^{\alpha} - F_{Zr}^{\alpha} \simeq RT \ln (1-2x)(1-x)^{-1} \tag{54}$$

$$\bar{F}_N^{\alpha} - 1/2F_{N_2}^G = -1/2F_{N_2}^G - 84,000 + RT \ln 665/T + RT \ln x(1-2x)^{-1} \tag{55}$$

Calculation of the $x_{\alpha\beta}$ vs T curve from Eq. 54 agrees very well with Fig. 24, Kibler, Lyon, and DeSantis[47] have measured the vapor pressure of nitrogen over the ZrN^{σ} phase at $1800 \leq T \leq 2300^{\circ}K$ and $0.415 < x < 0.489$. They suggest that $x_{\sigma\alpha}$ is less than 0.415 over the entire range of temperatures in contrast to Fig. 24. Estimating $x_{\sigma\alpha} \sim 0.40$ and equilibrating the partials of Zr and N across the $\alpha + \sigma$ field yields

$$F_{N+} \simeq 90,000 - 23.3T \tag{56}$$

and

$$F_{Zr+} + 2RT\ln 2\alpha = -3400 + 1.5T \tag{57}$$

Eq. (57) can be used to calculate the vapor pressure of nitrogen as a function of composition since (Eqs. 2, A1-12)

$$\bar{F}_N^{\sigma}[x] - 1/2F_{N_2}^{G} = 1/2\,RT\ln p_{N_2}^{\sigma}[x] = -F_{N+} + RT\ln x(1-2x)^{-1} \tag{58}$$

where $p_{N_2}^{\sigma}[x]$ is the pressure of nitrogen gas (in atmospheres). Performing these calculations yields good agreement at the low nitrogen end ($x = 0.415$) where the observed values are one and one half times the calculated values. At the high nitrogen end ($x = 0.489$) the observed value is twelve times the calculated pressure. The results of this calculation are given in Table III.

If the high nitrogen limit of the ZrN^{σ} phase is taken to be $x_{\sigma N} \sim 0.53$ as in the TiN^{σ} phase then

$$F_{Zr+} \sim 56,200 - 1.25T \tag{59}$$

and

$$RT\ln\alpha \sim -29,800 \tag{60}$$

Thus, the Zr-N and Ti-N cases yield values of $RT\ln\alpha$ for the σ phase intermediate between the carbide and oxide cases. The calculations show that the free energies of vacancy formation decrease with increasing temperature for each of the systems examined. Table IV contains a summary of values obtained for the vacancy parameter.

TABLE III

COMPARISON OF CALCULATED VAPOR PRESSURE OF NITROGEN OVER ZrN (Eq. 58) AND VALUES MEASURED BY Kibler, Lyon, and DeSantis[47] AS A FUNCTION OF COMPOSITION AT 2000°K.

x (at. fr. N)	$1/2 \log p_{N_2}$ (observed)	$1/2 \log p_{N_2}$ (Calc.)
0.489	-2.30	-2.90
0.485	-2.69	-3.34
0.480	-2.97	-3.67
0.470	-3.32	-3.86
0.455	-3.64	-4.05
0.440	-3.92	-4.15
0.415	-4.16	-4.36

TABLE IV

CALCULATED VALUES OF THE VACANCY PARAMETER FOR SEVERAL NaCl TYPE PHASES

PHASE	$-RT \ln \alpha/(1-2\alpha)$ (Cal/g. at.)
ZrC	44,100
TiC	43,850
TaC	38,500
ZrN	29,800
TiN	24,700
TiO	8,200

α = number of vacant metal (or non-metal) sites divided by the total number of sites at stoichiometry.

2α = number of vacant metal (or non-metal) sites divided by the number of metal (or non-metal) sites at stoichiometry.

3.0 X-Ray Debye Temperatures of HfC and ZrC

One of the essential ingredients in the thermodynamic analysis of the phase equilibria of a binary system is a knowledge of the room temperature entropy S[298] of a given compound A_nB_m. If one knows the experimental value of S[298], one can calculate a Debye temperature parameter by one of two methods:

$$S[298] = S_D[\frac{\overline{\theta}}{298}] \rightarrow \overline{\theta} \tag{61}$$

$$S[298] = \frac{n}{n+m} S_D[\frac{\theta_A}{298}] + \frac{m}{n+m} S_D[(\frac{M_B}{M_A})^{1/2} \frac{\theta_A}{298}] \rightarrow \theta_A = (\frac{M_B}{M_A})^{1/2} \theta_B \tag{62}$$

The first technique assumes the existence of some average Debye temperature $\overline{\theta}$ which can then be used to calculate the specific heat or entropy by using tabulated Debye functions $S_D[\frac{\theta}{T}]$. Electronic specific heat and $C_p - C_v$ corrections are assumed negligible here. The second "two Debye θ" approach is based on the empirical observation that two θ's associated with the individual atomic species often yield a more accurate calculated specific heat curve when compared with experimental data than does the average θ. Since θ_A and θ_B are not independent, either quantity is uniquely determined by S[298].

When data is not available, a direct measurement of $\overline{\theta}$ or θ_A and the use of the Debye functions corresponding to either method will yield specific heat or entropy curves. The calculated value of S[298] compared with the experimental value is considered to be a relatively sensitive test of the accuracy of any particular approach. The previous experimental x-ray study (ASD-TR-61-445) of a group of NaCl type compounds in which both $\overline{\theta}$ and θ_A were measured and calculated values of S[298] compared with published values was inconclusive. The small x-ray intensity changes resulting from the temperature change between

about 200°C and liquid nitrogen temperatures led to experimentally uncertain values of the Debye temperature. The present experimental program is an attempt to extend the intensity measurements to a high temperature range between 800°C and 1500°C relative to room temperature. The intensity changes for this range of temperature are quite large and the resulting θ's should be more accurate.

HfC and ZrC have been examined. Since good thermodynamic data is available for ZrC and the compounds are assumed to be similar, the results for ZrC can be compared with the data to check the validity of the measurement while the results for HfC can be used to predict specific heat and entropy curves.

Thermal expansion coefficients for the two carbides are also presented. In the process of obtaining the high temperature intensity plots, the angular shift of the diffraction peaks are also observed as a function of temperature. Thermal expansion of the lattice constant is then directly determined.

The analysis of the measured temperature dependence of the integrated x-ray peak intensities from powder specimens of the interstitial compounds HfC and ZrC is based on the following assumptions:

1) The mean square thermal displacements of the individual metal and non-metal atoms are effectively equal to a common isotropic displacement.
2) The temperature dependence of the observed peaks can be expressed in terms of a Debye temperature appropriate to an artificial monatomic lattice of mass equal to the average atomic mass of the two atoms or that of the metal atom.

The first assumption is suggested by both experimental observation and physical argument. The physical argument is based on the fact that HfC and ZrC

are high melting point compounds. This implies a relatively "stiff" lattice with strong interatomic bonding. Although different amplitudes of vibration for the individual atoms are possible because a diatomic lattice permits optical as well as acoustical modes, the strong interatomic bonding suggests that equivalent force fields act upon each atom to make the thermal amplitudes approximately equal. Experimentally, Houska[48] has measured the individual thermal amplitudes of Zr and C in ZrC and found the assumption of equal amplitudes valid within experimental uncertainty. The expression for the integrated peak intensity of a ZrC powder specimen having the NaCl structure is:

$$J_{\pm}[\phi, T] = f_{Zr}[\frac{\sin\phi}{\lambda}]\, e^{-8\pi^2\overline{\mu_{Zr}[T]}^2} \pm f_{C}[\frac{\sin\phi}{\lambda}]\, e^{-8\pi^2\overline{\mu_{C}[T]}^2} \qquad (63)$$

where $J_{\pm}[\phi, T] = \frac{I_{\pm}[\phi, T]}{p[hkl]\, L[\phi]\, K}$ is the normalized peak intensity. Here $I_{\pm}[\phi, T]$ is the observed, integrated, peak intensity at Bragg angle ϕ at temperature T, $p[hkl]$ the multiplicity factor for peaks of Miller indices {hkl}, $L[\phi]$ the Lorentz polarization factor, and K an instrument constant. f_{Zr} and f_C are the electronic scattering factors for the individual atoms and $\overline{\mu_{Zr}[T]}^2$ and $\overline{\mu_C[T]}^2$ are the corresponding mean square thermal amplitudes of vibration. The + sign is associated with all even Miller indices, the - sign with all odd indices; mixed indices are not allowed. If one plots $\ln(\frac{J_+ + J_-}{2f_{Zr}})$ and $\ln(\frac{J_+ - J_-}{2f_C})$ against $\frac{\sin^2\phi}{\lambda^2}$ at fixed temperature then the negative slopes of the resulting lines yield $\overline{\mu_{Zr}}^2$ and $\overline{\mu_C}^2$ respectively. Because the scattering power of the metal atom is larger than that of the non-metal atom, the determination of $\overline{\mu_C}^2$ is less certain.

In the present study, a similar analysis was performed for HfC and, again, no substantial difference in thermal amplitude could be found.

The second assumption that the compounds can be treated as artificial, monatomic, Debye solids can be verified if the intensity data over a large temperature range yields an essentially constant Debye temperature parameter for a choice of either average mass $\overline{M}$ or metal atom mass M_{Zr} or M_{Hf}. When the metal mass is chosen, the model is one of a sublattice of heavy atoms imbedded in a carbon continuum. The relationship between Debye θ and intensity I for a specific peak (hkl) is:

$$\ln\left(\frac{I_o}{I_T}\right) = \frac{\beta n^2}{M a_o^2 T_o} f[\gamma, x_o] \tag{64}$$

where $f[\gamma, x_o] = \frac{1}{x_o}\{G[\gamma x_o] - G[x_o]\}$ (65)

$$G[x] = \frac{1}{x^2}\int_o^x \frac{y\,dy}{e^y - 1} \tag{66}$$

$$\beta = \frac{3h^2 N_o}{k} = 5.73 \times 10^{-13} \text{ c.g.s.}$$

$$n^2 = h^2 + k^2 + l^2$$

$$\gamma = \frac{T_o}{T}, \quad x_o = \frac{\theta}{T_o} \qquad \begin{matrix} M = \overline{M}, & \theta = \overline{\theta} \\ M = M_A, & \theta = \theta_A \end{matrix}$$

a_o is the lattice constant, M the atomic weight, N_o Avogadro's number and all temperatures are expressed in ^oK. The function $f[\gamma, x_o]$ has been tabulated (ASD-TR-61-445 pt. II) for fixed values of γ so that high temperatures T are preselected once the reference temperature T_o (24°C in our case) is given. Thermal expansion has the effect of changing a_o with temperature; however, this correction was found to be negligible over the temperature range involved.

3.1 Experimental Results

The x-ray apparatus consisted of a Picker, horizontal diffractometer provided with a bent silicon crystal monochromator and an evacuated, high temperature specimen chamber. The carbide specimens were obtained from A.D. MacKay, Inc. with reported purities of >99.8[a]/o. Both lattice parameters a_o were measured to four figure accuracy by extrapolation techniques. For HfC, we obtain $a_o = 4.621$Å to be compared with 4.641Å reported for $HfC_{1.0}$ and 4.61Å for the Hf-HfC phase limit[48]. For ZrC, we obtain $a_o = 4.695$ to be compared with $a_o = 4.702$ for $ZrC_{0.95}$ and $a_o = 4.691$ for $ZrC_{0.55}$[48]. Both materials lie on the metal rich side of stoichiometry. 325 mesh specimen powder was deposited directly on a tantalum heating strip whose temperature was monitored with a calibrated optical pyrometer through a quartz window. A beryllium window provided access to the specimen for monochromated CuK_α radiation. Conventional scintillation counter and pulse height analyzer electronics were used to display diffraction peaks whose integrated intensities were measured graphically with a planimeter. Small specimen size and primary beam intensity loss from crystal monochromation led to low intensity peaks at the higher Bragg angles. The improved signal-to-background signal from monochromation, however, was sufficient to offset the difficulty of measuring low intensity peaks and relatively small intensity changes with temperature.

The thermal expansion results are given in TABLE V. Three lines each of ZrC and HfC were observed in the temperature range 800°C to 1500°C at 100°C intervals. In all cases, the angular shift with temperature was found to be linear, so that α, the linear expansion coefficient, could be extracted directly from the slope of each $\Delta\phi$ vs. T line. A specimen of pure Ta powder was employed initially to calibrate the apparatus and the resulting data from the Ta

powder indicated that extraneous thermal displacements of the apparatus in this temperature range would introduce errors not in excess of 5%. The expansion coefficient, α, is related to the slope, $\frac{d(\Delta\phi)}{dT}$, of the expansion curve by:

$$\alpha = \frac{\pi}{180} \cot\phi_o \frac{d\Delta\phi\,(deg)}{dT} \tag{67}$$

TABLE V

EXPANSION COEFFICIENTS FOR HfC AND ZrC

HfC

line	$(\phi_o(deg)$	$\frac{d\Delta\phi}{dT}$	α (/°C)
(440)	70.55	1.02×10^{-3}	6.29×10^{-6}
(422)	54.60	$.540 \times 10^{-3}$	6.70×10^{-6}
(420)	48.19	$.441 \times 10^{-3}$	6.86×10^{-6}

average $\alpha = 6.62 \times 10^{-6}/°C$

ZrC

(440)	68.11	1.25×10^{-3}	8.75×10^{-6}
(422)	53.47	$.730 \times 10^{-3}$	8.45×10^{-6}
(420)	47.18	$.502 \times 10^{-3}$	8.09×10^{-6}

average $\alpha = 8.43 \times 10^{-6}/°C$

The expansion coefficient for ZrC, $\alpha = 8.43 \times 10^{-6}/°C$ can be compared with a measurement by Houska[49] between 754°C and 1545°C, namely $\alpha = 7.20 \times 10^{-6}/°C$.

Debye temperature results are given in TABLE VI. The data was obtained for HfC by measuring the temperature dependence of the (440), (422) and (420) lines under CuK_α radiation at four temperatures above room temperature, 24°C. For ZrC, six temperatures and two lines (422) and (331) were used. Since these compounds exhibit cubic symmetry, the θ's obtained for any line should be the same. Consequently each number listed in TABLE VI is the averaged result at that temperature of two or three lines. The results from line to line do not differ by more than about 50°K; however the variation in θ from temperature to temperature is unexpectedly large for HfC. Between 830°C and 1350°C, both $\overline{\theta}$ and θ_{Hf} decrease by about 100°K whereas the θ's for ZrC are constant over this temperature range within experimental error. θ is expected to decrease with increasing temperature because the atomic volume is increasing. The Gruneisen relation predicts a decrease in Debye temperature of $\Delta\theta = 3\theta_1\alpha\gamma(T_2-T_1) = \theta_1-\theta_2$ where γ is the Gruneisen constant. For HfC, $\alpha \sim 7 \times 10^{-6}$, $\theta \sim 400$ and $\gamma \sim 2-3$ for most metallic solids. This predicts a $\Delta\theta$ of only about 10°K. The temperature average of $\overline{\theta}$ and θ_{Hf} are given as 440°K and 313°K for S[298] determinations. Houska[49] measured $\overline{\theta} = 587$°K for ZrC over the range 25°C to 1680°C, which is considerably higher than our value of $\overline{\theta} = 435$°K. Because the θ's for ZrC are relatively constant over the temperature range considered, we conclude that ZrC behaves more like a Debye solid than does HfC.

TABLE VII contains the calculated room temperature entropies using both $\overline{\theta}$ in equation 61 and θ_A in equation 62. Since the θ_A, θ_B method gives better agreement with the measured S[298] for ZrC[50], we predict that S[298] for HfC should be closer to 4.68 than to 5.92 $\frac{\text{cal}}{\text{g.at.}^\circ\text{K}}$.

TABLE VI

DEBYE TEMPERATURES FOR HfC AND ZrC

HfC

Temperature	830°C	907°C	1107°C	1350°C
$\bar{\theta}$	546°K	439°K	382°K	350°K
θ_{Hf}	380°K	323°K	282°K	267°K

average for $\bar{\theta}$ = 440°K

average for θ_{Hf} = 313°K, θ_C = 1205°K

ZrC

Temperature	915°C	1115°C	1212°C	1359°C	1474°C
$\bar{\theta}$	470°K	419°K	427°K	430°K	429°K
θ_{Zr}	350°K	315°K	318°K	326°K	321°K

average for $\bar{\theta}$ = 435°K

average for θ_{Zr} = 326°K, θ_C = 897°K

TABLE VII

ROOM TEMPERATURE ENTROPIES($\frac{\text{cal}}{\text{g. at. °K}}$ at 298)

FOR HfC AND ZrC

	$\bar{\theta}$ method	θ_A, θ_B method	measured[50]
ZrC	5.99	5.05	4.01
HfC	5.92	4.68	———

4.0 Estimation of the Free Energy of Formation of Hafnium Carbide

The free energy of formation of stoichiometric hafnium carbide, $\Delta F^{\circ}[T]$, in units of cal/g.at. can be approximated as follows:

$$\Delta F^{\circ}[T] = \Delta H^{\circ}[0^{\circ}K] + \Delta F_T^{\circ}[T] \tag{68}$$

In Eq. (68), $\Delta H^{\circ}[0^{\circ}K]$ is the enthalpy of formation at $0^{\circ}K$, while $\Delta F_T^{\circ}[T]$ is defined by Eq. (69),

$$\Delta F_T^{\circ}[T] = \int_o^T \Delta C_p \, dT - T \int_o^T T^{-1} \Delta C_p \, dT \tag{69}$$

where ΔC_p is the specific heat of the stoichiometric compound in cal/g.at.$^{\circ}K$ minus one half the sum of specific heats of hafnium metal and graphite in cal/g.at.$^{\circ}K$.

A preliminary value for $\Delta H^{\circ}[298^{\circ}K]$ has been obtained by K. K. Kelly by using combustion calorimetry. This value (quoted on p. 63 of 15 June 1963 report on contract AF33(657)-8223, H. L. Schick et al AVCO Corp., Wilmington, Mass.), which is subject to modification by Kelley, has been reported as -29.5 kcal/g.at. or -59.0 kcal/mol. Since ΔH° will not vary by more than 200 cal/mol between $0^{\circ}K$ and $298^{\circ}K$, the latter value can be safely adapted for $\Delta H^{\circ}[0^{\circ}K]$ i.e.

$$\Delta H^{\circ}[0^{\circ}] \approx -29.5 \text{ kcal/g.at.} \tag{70}$$

$$2\Delta H^{\circ}[0^{\circ}K] \approx -59.0 \text{ kcal/mol} \tag{71}$$

Consequently, specification of $\Delta F^{\circ}[T]$ requires that $\Delta F_T^{\circ}[T]$ be evaluated.

Since no low temperature specific heat data are available for HfC, the x-ray results obtained in section 3.0 of this report will be used to estimate $\Delta F_T^{\circ}[T]$. This procedure requires considering the vibrational, electronic specific heat, and phase change components of hafnium, carbon, and hafnium carbide to $\Delta F_T^{\circ}[T]$.

4.1 Hafnium

Walcott[51] has measured the specific heat of hafnium between 4°K and 300°K. He suggests, $\theta_{Hf} = 200°K$, and $\gamma_{Hf} = 6.3 \times 10^{-4}$ cal/g.at. $°K^2$. Hafnium undergoes a h.c.p. → b.c.c. transition on heating above 2033°K. We can approximate $\Delta S^{\alpha \to \beta}$, i.e., the entropy change for the h.c.p. → b.c.c. transition as 0.9 cal/g.at.°K on the basis of earlier work on Ti and Zr[1]. The melting point of Hf is 2495°K, and we approximate $\Delta S^{\beta \to L} = 2.1$ cal/g.at.°K.

4.2 Graphite

The free energy function for the graphitic form of carbon is tabulated by Janaf and by Elliot and Gleiser[26]. These data can be used to compute $F_C^\circ [T]$.

4.3 Hafnium Carbide

Westrum[50] has measured the specific heat of ZrC between 5°K and 350°K. Plotting his low temperature data (5-25°K) as Cp/T vs T^2 yields a very low value of γ for ZrC (i.e., $\gamma \simeq 0.5 \times 10^{-4}$ cal/g.at. $°K^2$). Similar values have been noted for the refractory borides ZrB_2, TiB_2 and HfB_2. On the basis of section 3.0, we approximate $\theta_{Hf}^0 = 313°K$ and $\theta_C^0 = 1205°K$ for HfC.

On the basis of this information $\Delta F_T^0 [T]$ can be computed as follows: For hafnium, we evaluate $F_{Hf}^\circ [T]$ by using Eq. (72)

$$F_{Hf}^\circ [T] = F[\tfrac{\theta}{T}] + 10^{-4}(3R\theta^2 P - T\,U[\tfrac{\theta}{T}]) - \gamma_{Hf} T^2/2 + \Delta F_{Hf}^{\alpha \to \beta}[T] + \Delta F_{Hf}^{\beta \to L}[T] \qquad (72)$$

where

$$P = T^2/2\theta^2 - (1/40) \ln (1 + 20\,T^2/\theta^2) \qquad (73)$$

and $F[\frac{\theta}{T}]$ and $U[\frac{\theta}{T}]$ are the Debye free energy and energy functions. These equations derive from the approximation*

$$C_p = C_v [\tfrac{\theta}{T}] \; (1 + 10^{-4} T) + \gamma T \qquad (74)$$

*Recent high temperature measurements (1200-3000°K)[52] on NbC and TaC offer further support for this approximation.

where $\theta = 200^{\circ}K$, and $\gamma = 6.3 \times 10^{-4}$ cal/g.at $^{\circ}K^2$. The first term on the right of Eq. (72) is the vibrational free energy term[1] (at constant volume), the second term arises from the $(C_p - C_v)$ correction which is approximated by $10^{-4} T\, C_v \left[\frac{\theta}{T}\right]$ in Eq. (74). The third term is the electronic specific heat contribution to the free energy. The fourth term, which is added only for $T > 2033^{\circ}K$ is given by

$$\Delta F_{Hf}^{\alpha \to \beta} \simeq -0.9\,(T - 2033^{\circ}K) \text{ cal/g.at.} \tag{75}$$

while the fifth term which is added only for $T > 2495^{\circ}K$ is

$$\Delta F_{Hf}^{\beta \to L} \simeq -2.1\,(T - 2495^{\circ}K) \text{ cal/g.at.} \tag{76}$$

A similar procedure can be used for to compute $F_T^{\sigma}[T]$ for HfC. by using an expression similar to Eq. (72) with $\theta_{Hf}^{\sigma} = 1205\,^{\circ}K$ and $\gamma \sim 0$ i.e.

$$2F_T^{0}[T] = F\left[\frac{313}{T}\right] + F\left[\frac{1205}{T}\right] + 3 \times 10^{-4} R\left((313)^2 P[313] + (1205)^2 P[1205]\right)$$

$$- 10^{-4} T\left(U\left[\frac{313}{T}\right] + U\left[\frac{1205}{T}\right]\right) \text{ cal/mol} \tag{77}$$

Since

$$2\Delta F_T^{0}[T] = 2F_F^{0}[T] - F_{Hf}^{o}[T] - F_C^{o}[T] \tag{78}$$

Performing the numerical calculations of Eqs. (72) to (78) and combining with Eqs. (71) and (68) yields the values for the free energy of formation which are tabulated in Table VIII. These values have been used in connection with the calculations of vapor pressure and phase equilibria

presented in section 2.0. (See pp. 22, 28, 29, 36, and 37.) In view of the agreement shown in Figs. 18 and 19, it appears that the values in Table VIII are accurate to within 2 kcal/mol or better.

TABLE VIII

ESTIMATED VALUES FOR THE FREE ENERGY OF FORMATION OF STOICHIOMETRIC HAFNIUM CARBIDE

($2\Delta F^{0}[0.5, T]$ in kcal/mol)

$2\Delta H^{0}[0.5, 0^{\circ}K] \approx 2\Delta H^{0}[0.5, 298^{\circ}K] \approx -59.0$ kcal/mol

$T^{\circ}K$	$2\Delta F^{0}[T]$ (kcal/mol)
1400	-55.8
1600	-55.4
1800	-55.0
2000	-54.6
2200	-54.2
2400	-53.6
2600	-53.1
2800	-52.1
3000	-51.2
3200	-50.2
3400	-49.3
3600	-48.3
3800	-47.3
4000	-46.3

APPENDIX A1

EXPLICIT FORMULATION OF THE COMPOSITIONAL DEPENDENCE OF THE FREE ENERGY OF NON-STOICHIOMETRIC PHASES

In considering the thermodynamic properties of refractory oxide, carbide, and nitride compounds it is quite apparent that many of these compounds are not line compounds. In reality they are found to exist over a range of compositions at elevated temperatures and even at room temperature. Recently these deviations from stoichiometry have been recognized as contributing factors in controlling many of the important properties of these compounds. In order to proceed with the analysis of the thermodynamic properties of metal-nonmetal systems it is necessary to derive equations which can be used to explicitly define the thermodynamic properties of these nonstoichiometric compounds. This conclusion is apparent if one considers TiO, ZrC, TiN, or TaC as examples.

Schottky and Wagner[18] have formulated a generalized thermodynamic model of non-stoichiometric compounds. A detailed description of this general model is given by Wagner[19] in which one gram atom of a compound $A_{(1-x)}B_x$ is considered. In the present notation x is the atomic fraction of element B (rather than Wagner's symbol x_2). The general model allows for two sublattice, an A sublattice and a B sublattice, which contain both A and B vacancies, A and B interstitials, A atoms on B lattice sites and B atoms on A lattice sites. Restricting consideration to the interstitial type compounds of interest i.e., where the B atom is much smaller than the A atom and the B sublattice fits within the interstices of the A sublattice, the general model can be restricted.

As a first approximation we consider the case where the only defects present are vacant A sites and vacant B sites.

We consider a compound $A_{(1-x)}B_x$ which has the δ crystal structure with a composition range about x_o. Thus the compound is ideally $A_{(1-x_o)}B_{x_o}$, but can exist for values of x greater than x_o (corresponding to an excess of vacant A sites) or less than x_o (corresponding to and excess of vacant B sites). Since we consider a gram atom of compound then the number of A atoms is given by Eq. (A1-I) as

$$N(1-x) = (1-x_o)\,N_s - N_{A+} \qquad \text{(A1-I)}$$

where N is Avogadro's number, N_s is the total number of lattice sites (A sites plus B sites) and N_{A+} is the number of A lattice sites which are vacant. The number of B atoms is given by Eq. (A1-2) as

$$Nx = x_o\,N_s - N_{B+} \qquad \text{(A1-2)}$$

where N_{B+} is the number of vacant B lattice sites. The ratio of the total number of sites N_s to the total number of atoms, N_s/N, is set equal to a parameter y. Hence the fraction of vacant sites is

$$(N_s - N)/N_s = (1 - 1/y) \qquad \text{(A1-3)}$$

The free energy of the δ phase as a function of temperature and composition (reference (19) equations (3-1)-(3-8)) is given as

$$F^{\delta}[T,x] = (1-x)\,F_A^o[T] + xF_B^o[T] + (N_{A+}/N)F_{A+}[T]$$

$$+(N_s/N)(F^{*\delta}[T] - (1-x_o)F_A^o[T] - x_oF_B^o[T]) + (N_{B+}/N)F_{B+}[T]$$

$$+kT\,\{N_{A+}\ln(N_{A+}/(1-x_o)N_s) + N_{B+}\ln(N_{B+}/x_oN_s)$$

$$+((1-x_o)N_s - N_{A+}) \ln((1-x_o)\ N_s - N_{A+})/(1-x_o)N_s$$

$$+ (x_o N_s - N_{B+}) \ln (x_o N_s - N_{B+})/x_o N_s \} \qquad \text{(A1-4)}$$

These equations apply for the case where $F_A^o[0^oK]$ and $F_B^o[0^oK]$, which are the free energies of one gram atom of A and B respectively at one atmosphere pressure, are equal to zero at 0^oK, and all of the free energies are understood to be temperature dependent. In these equations F_{A+} and F_{B+} are the free energies of a gram atom of A and B vacancies.

For a given temperature, pressure and composition i.e. (N_A and N_B are constant), the free energy F^δ is a minimum when†

$$-RT \ln \alpha = F_{*}^{\delta}[x_o] - (1-x_o)(F_A^o - F_{A+} + RT \ln (1-x_o)) - x_o(F_B^o - F_{B+} + RT \ln x_o) \qquad \text{(A1-5)}$$

and

$$\ln \alpha = (1-x_o) \ln((1-x_o)\ y + x - 1)/y + x_o \ln (x_o y - x)/y \qquad \text{(A1-6)}$$

Substitution of these expressions into (A1-4) yields $F^\delta[T, x]$ given in TABLE A1-I. The partial molar free energies $\overline{F}_A$ and $\overline{F}_B$ are then derived by applying the general relations,

$$\overline{F}_A = F - x \frac{\partial F}{\partial x} \quad \text{and} \quad \overline{F}_B = F + (1-x) \frac{\partial F}{\partial x} \qquad \text{(A1-7)}$$

The equations given in Table A1-I should apply for situations where x is not very different from x_o, and the fraction of vacant sites, $(N_s - N)/N_s$, is small for $x = x_o$ i.e., $(y-1)$ is small at $x = x_o$. Under these conditions,

---

† $F_{*}^{\delta}[x_o]$ is the free energy of one gram atom of vacancy free stoichiometric-compound

TABLE A1-I

THERMODYNAMIC EQUATIONS FOR ONE GRAM-ATOM OF NONSTOICHIOMETRIC COMPOUND $A_{(1-x_o)}B_{x_o}$ WHICH HAS THE δ STRUCTURE

x	= atom fraction B	N_{A+}	= number of vacant A sites
N	= Avogadro's Number	N_{B+}	= number of vacant B sites
N_s	= total number of lattice sites	y	$= N_s/N,\ y \geq 1$

General Case

$$N(1-x) = (1-x_o)\,N_s - N_{A+} \qquad Nx = x_o N_s - N_{B+}$$

$$F^{\delta} = (1-x)\,F_A^o + xF_B^o + y(F_*^{\delta}[x_o] - (1-x_o)F_A^o - x_o F_B^o) + ((1-x_o)y-(1-x))F_{A+}$$

$$+(x_o y-x)F_{B+} + RT((y(1-x_o) + x-1)\ln((1-x_o)y+x-1)/y(1-x_o)$$

$$+(x_o y-x)\ln(x_o y-x)/x_o y + x\ln x/x_o y$$

$$+(1-x)\ln(1-x)/(1-x_o)y)$$

$$\overline{F}_B^{\delta} = F_B^o - F_{B+} + RT\ln x/(x_o y-x)$$

$$\overline{F}_A^{\delta} = F_A^o - F_{A+} + RT\ln(1-x)/((1-x_o)y+x-1)$$

where

$$\ln\alpha = (1-x_o)\ln((1-x_o)y + x-1)/y + x_o\ln(x_o y-x)/y$$

and

$$-RT\ln\alpha = F_*^{\delta}[x_o] - (1-x_o)(F_A^o - F_{A+} + RT\ln(1-x_o)) - x_o(F_B^o - F_{B+} + RT\ln x_o)$$

hence

$$\Delta F^{\delta} = \Delta F_*^{\delta} + RT\ln(1-\alpha\, x_o^{-x_o}(1-x_o)^{(x_o-1)})$$

TABLE A1-I (Continued)

when $x = x_o$

$$\alpha = x_o^{x_o}(1-x_o)^{1-x_o}(1-1/y) = x_o^{x_o}(1-x)^{1-x_o}(N_s-N)/N_s$$

and

$$N_{A+} = x_o(N_s-N);\ N_{B+} = (1-x_o)(N_s-N)$$

Special Case

$$x_o = 0.5, \qquad A_{0.5}B_{0.5}$$

$$N(1-x) = 0.5\,N_s - N_{A+}, \qquad Nx = 0.5\,N_s - N_{B+}$$

$$F^{\delta} = (1-x)F_A^o + xF_B^o + y(F_*^{\delta}[0.5] - 0.5\,F_A^o - 0.5\,F_B^o) + (0.5\,y-x)\,F_{B+}$$

$$+(0.5y+x-1)\,F_{A+} + RT\,((0.5y+x-1)\ln(0.5y+x-1)/0.5y + x\ln x/0.5y$$

$$+(0.5y-x)\ln(0.5y-x)/0.5y + (1-x)\ln(1-x)/0.5y)$$

$$\bar{F}_A^{\delta} = F_A^o - F_{A+} + RT\ln(1-x)/(0.5y-(1-x))$$

$$\bar{F}_B^{\delta} = F_B^o - F_{B+} + RT\ln x/(0.5y-x)$$

where $-RT\ln\alpha = F_*^{\delta}[0.5] - 0.5(F_A^o + F_B^o - F_{A+} - F_{B+}) - RT\ln 0.5$

and $y = (1-4\alpha^2)^{-1}(1+(1-4x(1-x)(1-4\alpha^2))^{1/2})$

when $x = 0.5$, $y = 1/(1-2\alpha)$, and $N_{A+}/N_s = N_{B+}/N_s = \alpha = 0.5\,(N_s-N)/N_s$

$$\Delta F^{\delta}[0.5] = \Delta F_*^{\delta}[0.5] + RT\ln(1-2\alpha)$$

$$F_{*}^{\delta}[x_o] - (1-x_o)F_A^o - x_oF_B^o$$

is the free energy of formation of one gram atom of the stoichiometric compound. For a fixed number of A and B atoms (i.e. a fixed value of x), F^{δ} given in Table A1-I is a minimum when y takes on a specific value. This value of y is specified by means of the parameter α in terms of F_{A+}, F_{B+}, and the free energy of formation of the ideally ordered compound $F_{*}^{\delta}[x_o]$, (for which $y=1$).

The equations for the case of a general value of x_o are simplified considerably if we consider a special case when $x=0.5$ i.e., TiO, TiN, ZrC etc.

In this case we see that α is equal to the fraction of vacant A lattice sites (and the fraction of vacant B lattice sites) at $x=0.5$. The equations for the partial molar free energies of A and B are complicated by the fact that y is a complex function of x even for the special case of $x_o=0.5$. However, if we recognize that α (which is the fraction of vacant A or B sites at $x=0.5$) is small then the expression for y can be simplified. The usual values for α are considerably less than 1%. If we restrict consideration to the situation where α is very much less than unity then

$$(N_s/N) = y = 1 \pm ((1-2x) \qquad \text{(A1-8)}$$

since y must be greater than unity the plus sign refers to $x<0.5$ and the minus sign to $x>0.5$ in eq. A1-8. Under these conditions the following expressions result: at $x = 0.5$

$$\overline{F}_A^{\delta} = F_A^o - F_A^+ + RT\ln(1-2\alpha)/2\alpha \qquad \text{(A1-9)}$$

$$\overline{F}_B^{\delta} = F_B^o - F_B^+ + RT\ln(1-2\alpha)/2\alpha \qquad \text{(A1-10)}$$

Eqs. (A1-9 and A1-10) apply even when α is not small.

When $x < 0.5$ (and $\alpha^2/(1-2x)^2$ is very small) then

$$\bar{F}_A^{\delta} = F_A^{o} - F_{A+} + RT \ln(1-2x)/4(1-x)\alpha^2 \qquad (A1-11)$$

$$\bar{F}_B^{\delta} = F_B^{o} - F_{B+} + RT \ln x/(1-2x) \qquad (A1-12)$$

while for $x > 0.5$

$$\bar{F}_A^{\delta} = F_A^{o} - F_{A+} + RT \ln(1-x)/(2x-1) \qquad (A1-13)$$

$$\bar{F}_B^{\delta} = F_B^{o} - F_{B+} + RT \ln(2x-1)/4x\alpha^2 \qquad (A1-14)$$

If $a_A[x]$ and $a_A[x_o]$ are the activities of A at a composition x and at $x_o = 0.5$ then for $x<0.5$ the ratio of activities (or vapor pressures) is

$$a_A[x]/a_A[x_o] = (1-2x)/2(1-x)\alpha \qquad (A1-15)$$

and

$$a_B[x]/a_B[x_o] = 2\alpha x/(1-2x) \qquad (A1-16)$$

Thus the activity of A <u>increases</u> while the activity of B <u>decreases</u> with increasing deviation from stoichiometry. On the other hand, when $x > x_o$.

$$a_A[x]/a_A[x_o] = 2\alpha(1-x)/(2x-1) \qquad (A1-17)$$

and

$$a_B[x]/a_B[x_o] = (2x-1)/2x\alpha \qquad (A1-18)$$

so that the activity of A <u>decreases</u> and the activity of B <u>increases</u> with increased deviation from stoichiometry. This is the general behavior to be expected for such compounds.

At this point it is worthwhile introducing a simplification by inserting the relation between α, F_{A+}, and F_{B+} into the equations for $\bar{F}_A$ and $\bar{F}_B$. If we

let $\Delta F_f[x_o, T]$ be the free energy of formation of one gram atom of the compound i.e.*

$$\Delta F_f[x_o, T] = F^{\delta}[x_o] - (1-x_o) F_A^o - x_o F_B^o \qquad \text{(A1-19)}$$

then

$$-2RT \ln\alpha = 2\Delta F_f[x_o, T] + F_{A+} + F_{B+} + 2RT \ln 2 \qquad \text{(A1-20)}$$

Hence from eqs. (A1-11-15) we find, (with $x_o = 1/2$)

for $x < 0.5$

$$\bar{F}_A^{\delta} = F_A^o + 2\Delta F_f[1/2, T] + F_{B+} + RT \ln(1-2x)/(1-x) \qquad \text{(A1-21)}$$

$$\bar{F}_B^{\delta} = F_B^o - F_{B+} + RT \ln x/(1-2x) \qquad \text{(A1-22)}$$

and

$$\bar{F}_A^{\delta} = F_A^o - F_{A+} + RT \ln(1-x)/(2x-1)$$

$$\bar{F}_B^{\delta} = F_B^o + 2\Delta F_f[1/2, T] + F_{A+} + RT \ln(2x-1)/x \qquad \text{(A1-23)}$$

for $x > 0.5$.

These expressions can be used to calculate the compositional variation of the enthalpy of formation of the δ phase at 298°K. If α is small (which is probably likely at low temperatures) then the enthalpy of formation, ΔH_f, is given by

$$\Delta H_f = H^{\delta} - (1-x) H_A^o - x H_B^o = y\Delta H_* + (y/2 + x - 1) H_{A+} + (y/2 - x) H_{B+} \qquad \text{(A1-24)}$$

where ΔH_* is the enthalpy of formation at stoichiometry. For x less than 0.5

---

*Note that these approximations apply only when $F^{\delta}[x_o] \cong F_*^{\delta}[x_o]$ or when α is very small. If this is not so, then a more exact expression, namely $F^{\delta}[x_o] = F_*^{\delta}[x_o] + RT \ln(1-2\alpha)$ results.

(i.e. $y=2(1-x)$) then

$$\Delta H_f - \Delta H_{\ast} \approx (1-2x)(\Delta H_{\ast} + H_{B+}) \qquad (A1-25)$$

while when x is greater than $0.5\,(y-2x)$

$$\Delta H_f - \Delta H_{\ast} \approx (2x-1)(\Delta H_{\ast} + H_{A+}) \qquad (A1-26)$$

Application of these equations for the case where x_o is different from $1/2$ in the exact form is complicated by the fact that the solution for y in terms of α involves cubic or higher order equations. However some simplifications can be applied if α is very small.

Recasting Eq. A1-6 as:

$$(\alpha y)^{(1/x_o)} = (x_o y - x)(1-x_o)y + x - 1)^{-(1-1/x_o)} \qquad (A1-27)$$

indicates that when α is small, $y \sim x/x_o$ for $x > x_o$ and $y \sim (1-x)/(1-x_o)$ for $x < x_o$. These approximations can be used to write the analogues of Eqs. A1-9-14 for $x_o \neq 1/2$; thus at $x = x_o$ (for all values of α)

$$\bar{F}_A^{\delta} = F_A^o - F_{A+} + RT \ln(\alpha^{-1} x_o^{x_o} (1-x_o)^{(1-x_o)} - 1) \qquad (A1-28)$$

$$\bar{F}_B^{\delta} = F_B^o - F_{B+} + RT \ln(\alpha^{-1} x_o^{x_o} (1-x_o)^{(1-x_o)} - 1) \qquad (A1-29)$$

when α is small and $x < x_o$

$$\bar{F}_A^{\delta} = F_A^o - F_{A+} + (1-x_o)^{-1} RT \ln(1-x)^{-x_o} (1-x_o)^{(1-x_o)} (x_o - x)^{x_o} \alpha^{-1} \qquad (A1-30)$$

$$\bar{F}_B^{\delta} = F_B^o - F_{B+} + RT \ln x (1-x_o)(x_o - x)^{-1} \qquad (A1-31)$$

and when $x > x_o$

$$\bar{F}_A^{\delta} = F_A^o - F_{A+} + RT \ln x_o (1-x)(x-x_o)^{-1} \qquad (A1-32)$$

$$\bar{F}_B^{\delta} = F_B^{o} - F_{B+} + x_o^{-1} RT \ln x^{(x_o-1)} x_o^{x_o} (x-x_o)^{(1-x_o)} \alpha^{-1} \qquad \text{(A1-33)}$$

Similarly the compositional dependence of the enthalpy of formation is given by equations (A1-34-35) as:

$$\Delta H_f - \Delta H_* = (x_o - x)(1-x_o)^{-1}(\Delta H_* + H_{B+}) \qquad \text{(A1-34)}$$

for $x < x_o$, and

$$\Delta H_f - \Delta H_* = x_o^{-1}(x-x_o)(\Delta H_* + H_{A+}) \qquad \text{(A1-35)}$$

for $x > x_o$

APPENDIX A2

APPROXIMATION OF THE EXCESS FREE ENERGY OF MIXING OF INTERSTITIAL SOLID SOLUTIONS

Kaufman, Radcliffe, and Cohen[4] have formulated the compositional and temperature dependences of an α interstitial solid solution of element C in element A in which there exist n interstitial C sites per A site. In this model z-1 of the interstitial sites surrounding a given "C-site" are excluded from occupancy (by other C atoms) if it is filled by a C atom. In this situation, the α solution terminates at a composition corresponding to $x = n(n+z)^{-1}$ corresponding to a compound $AC_{n/z}$. The free energy of a gram atom of such a solution is defined by Eqs. 5-7 of reference (4). Moreover, the partial molar free energies are given in terms of Eqs. (7-8) of reference (4). In order to complete the explicit formulation of the free energy of the α solid solution, it is necessary to define the excess free energy of mixing F_E^{α} and the free energy of the terminal compound $AC_{n/z}$.

As a first approximation, $0^{\circ}K$ enthalpy contributions and changes in vibrational free energy are considered as the primary contributions to these terms. Restricting consideration to high temperatures, the vibrational free energy can be approximated by $3\,RT \ln \theta/T$ where θ is the Debye temperature. On the basis of these assumptions the free energy of a gram atom of $AC_{n/z}$ is:

$$F^{\alpha}_{AC_{n/z}}[T] = H^{\alpha}_{AC_{n/z}}[0^{\circ}K] + 3\,RT\left\{\left(1-\frac{n}{n+z}\right)\ln\frac{\theta_A^{*\alpha}}{T} + \frac{n}{n+z}\ln\frac{\theta_C^{*\alpha}}{T}\right\} \qquad \text{(A2-1)}$$

In Eq. (A2-1) $\theta_A^{*\alpha}$ and $\theta_C^{*\alpha}$ are the individual Debye Temperatures of A atoms and C atoms in the compound $\alpha AC_{n/z}$. According to the Two-Debye-θ method[5]

$$\theta_C = \theta_A M_A^{1/2} M_C^{-1/2} \tag{A2-2}$$

thus

$$\theta_C^{*\alpha} = \theta_A^{*\alpha} M_A^{1/2} M_C^{-1/2} \tag{A2-3}$$

In Eq. (A2-1), $H^{\alpha}_{AC_{n/z}}[0^{\circ}K]$ is the heat of formation of one gram atom of $\alpha AC_{n/z}$ from $(1-\frac{n}{n+z})$ gram atoms of αA and $\frac{n}{n+z}$ gram atoms of the S_o form of C at $0^{\circ}K$. Since the enthalpy of αA and the S_o form of C at $0^{\circ}K$ are both zero at $0^{\circ}K$, then in the spirit of the present approximation

$$F_A^{\alpha}[T] \simeq 3\,RT \ln \theta^{o\alpha}_{A/T} \tag{A2-4}$$

at high temperatures, where $\theta_A^{o\alpha}$ is the Debye temperature of pure αA.

Definition of F_E^{α} requires a division of F_E^{α} into two terms, a $0^{\circ}K$ term and a temperature dependent term. The simplest form of the $0^{\circ}K$ term is $Ax(1-x(n+z)n^{-1})$ which is zero at $x=0$ and $x=n(n+z)^{-1}$. If the Debye temperature of A and C are related by Eq. (A2-2) then:

(A2-5)

$$F_E^{\alpha}[x,T] = Ax\left(1-\frac{n+z}{n}x\right) + 3RT\left\{(1-x)\ln\frac{\theta_A^{\alpha}[x]}{\theta_A^{o\alpha}} + x\ln\left(\frac{\theta_C^{\alpha}[x]}{\theta_C^{*\alpha}}\right)\left(\frac{\theta_A^{o\alpha}}{\theta_A^{*\alpha}}\right)^{z/n}\right\}$$

where $\theta_A^{\alpha}[x]$ and $\theta_C^{\alpha}[x]$ are the Debye temperatures of elements A and C in the α solution at composition x, and A is a constant. On the basis of this definition, the chemical potentials of elements A and C, $\bar{F}_A^{\alpha}$ and $\bar{F}_C^{\alpha}$, in the α solid solution can be defined as (Eqs. 5-9 of ref. (4)) follows:

(A2-6)

$$\bar{F}_A^{\alpha} = F_A^{\alpha} + \frac{RTn}{z}\ln\frac{n-x(n+z)}{n(1-x)} + Ax^2\frac{(n+z)}{n} + 3RT\left\{\ln\frac{\theta_A^{\alpha}[x]}{\theta_A^{o\alpha}} - \frac{x}{\theta_A^{\alpha}[x]}\frac{d\theta_A^{\alpha}[x]}{dx}\right\}$$

and

$$\bar{F}_C^{\alpha} = \frac{n+z}{n}H^{\alpha}_{AC_{n/z}}[0^{\circ}K] + 3RT\ln\frac{\theta_C^{o\alpha}}{T} + RT\ln\frac{x}{n-(n+z)x} \tag{A2-7}$$

$$+A\left\{1-2x\frac{(n+z)}{n} + x^2\frac{(n+z)}{n}\right\} + 3RT\left\{\ln\frac{\theta_C^{\alpha}[x]}{\theta_C^{o\alpha}} + \frac{(1-x)}{\theta_C^{\alpha}[x]}\frac{d\theta_C^{\alpha}[x]}{dx}\right\}$$

Consequently, this formulation specifies the free energy of the interstitial solution in terms of n, which can be evaluated from a knowledge of the crystal structure (i.e. n = 1 for h.c.p. and f.c.c. lattices and 3 for b.c.c. lattices); the compositional dependence of the Debye temperatures A and C, which can be estimated from a knowledge of the melting point and volume[5]; the exclusion parameter z, which is equal to unity for an ideal interstitial solution; and the parameters A and $H^{\alpha}_{AC_{n/z}}[0^{\circ}K]$.

The enthalpy of formation of one gram atom of solution from (1-x) gram atoms of A^{α} and x gram atoms of the S_o form of C(the stable form at $0^{\circ}K$ and one atmosphere pressure) is,

$$\Delta H_f[x, 0^{\circ}K] = n^{-1}x(n+z)\, H^{\alpha}_{AC_{n/z}}[0^{\circ}K] + Ax(1-n^{-1}x(n+z)) \qquad (A2\text{-}8)$$

TABLE OF SYMBOLS

Several symbols used in this paper have more than one connotation. However in the few cases where two meanings are possible the proper choice is apparent from the text. It should be noted that brackets are used exclusively to denote functional relations. Thus $V^{\sigma}[x, T, P]$ is the volume of the σ phase which is a function of composition, x, temperature and pressure. As is indicated in the text, all vapor pressure and free energy terms are temperature dependent and free energies are discussed in units of calories per gram atom.

B	a pure element B.
C	a pure element C.
σ	a phase having the sodium chloride crystal structure.
β	a phase having the b.c.c. crystal structure.
γ	the "graphite" crystal structure.
L	the liquid phase.
T_{Me}^{β}	the melting point of the β form of a metal.
T_{Me}^{γ}	the melting point of the γ form of a metal.
T^{σ}	the melting point of the σ phase.
x	atomic fraction of non-metal (i.e. carbon, oxygen, nitrogen).
T_E	the eutectic temperature corresponding to a eutectic composition which is less than $x = 0.5$.
$x_{\beta\sigma}$	the composition of the $\beta/\beta+\sigma$ phase boundary.
$x_{\beta L}$	the composition of the $\beta/\beta+L$ phase boundary.
$x_{\sigma\beta}$	the composition of the $\sigma/\beta+\sigma$ phase boundary.

$x_{L\sigma}$	the composition of the L/L+ σ phase boundary for $x_{L\sigma}$ less than 0.5.
$x_{\sigma L}$	the composition of the σ/L+σ phase boundary for $x_{\sigma L}$ less than 0.5.
$\overline{x}_{L\sigma}$	the composition of the L/L+ σ phase boundary for $\overline{x}_{L\sigma}$ greater than or equal to 0.5.
$\overline{x}_{\sigma L}$	the composition of the σ/L+ σ phase boundary for $\overline{x}_{\sigma L}$ greater than or equal to 0.5.
F_A^{β}	the free energy of the β form of A which is (understood to be) a function of temperature.
$F^{\sigma}[x]$	the integral free energy of the σ phase which is a function of composition (and temperature).
$\overline{F}_A^{\sigma}[x]$	the partial molar free energy of A in the σ phase which is a function of composition and temperature.
$\overline{F}_A^{\sigma}{}_{x_{\sigma\beta}}$	the partial molar free energy of A in the σ phase evaluated at a composition corresponding to the boundary of the $\sigma/\sigma+\beta$ phase field.
F_C^{γ}	the free energy of the graphite, γ, form of carbon.
p_{Zr}^{β}	the vapor pressure of the β form of pure Zr.
$p_{Zr}^{\sigma}[x]$	the vapor pressure of Zr over the σ phase which is a function of composition (and temperature).
ΔF^{σ}	the free energy of formation of the σ phase at stoichiometry (cal/g.at.).
F_{Me+}	the free energy of formation of Me vacancies.
F_{C+}	the free energy of formation of C vacancies.
α	the phase α, or the vacancy parameter which is proportional to the fraction of vacant lattice sites at stoichiometry (See Table AI for mathematical definition).
$\Delta F_C^{\delta\rightarrow\gamma}$	the difference in free energy between the δ (diamond cubic) and γ (graphitic) forms of carbon.
$\Delta F_C^{\gamma\rightarrow L}$	the difference in free energy between the γ and liquid form of carbon.
$\Delta S_C^{\gamma\rightarrow L}$	the difference in entropy between the γ and liquid form of carbon.
N	Avogadro's number.
k	Boltzmann's constant.

R	the gas constant = 1.9873 cal/g.at. = Nk.
$\Delta F_{Me}^{L\rightarrow\beta}$	the difference in free energy between the β and liquid forms of a metal.
$\Delta H^{\sigma}[0^{\circ}K]$	the enthalpy of formation of one gram atom of σ phase of stoichiometric composition at $0^{\circ}K$.
G	the rate of Langmuir evaporation (mols/cm^2sec.).
x_C	the composition of congruent vaporization (i.e. $x_C = x_C[T]$).
$1/2F_{O_2}^{G}$	the free energy of one half mol (i.e. one gram atom), of oxygen gas at atmospheric pressure.
$\theta_{Ti}^{\alpha}[x]$	the Debye temperature of Ti in the α solid solution (which is a function of composition).
$H_{TiO}^{\alpha}[0^{\circ}K]$	the enthalpy of the α form of TiO at $0^{\circ}K$.
A	element A, or the enthalpy of mixing parameter for α interstitial solid solutions (see Eq. A2-5).
$\Delta F_{Ti}^{\alpha\rightarrow\beta}$	the free energy difference between the α and β forms of titanium.
$\theta_{Zr}^{o\alpha}$	the Debye temperature of pure α Zr i.e. $\theta_{Zr}^{\alpha}[x]$ at $x=0$.
N_s	the total number of lattice sites.
N_{A+}	the number of A lattice sites which are vacant.
y	the ratio of the total number of sites to the total number of atoms, N_s/N.
$F^{\delta}[T,x]$	the free energy of the δ phase which is a function of temperature and pressure.
$F_{*}^{\delta}[x_o]$	the free energy of one gram atom of vacancy free stoichiometric compound.
$a_A[x]$	the activity of element which is a function of composition and understood to be a function of temperature.
α interstitial solid solution	the interstitial solid solution of element C in element A.
n	the number of interstitial C sites per A atom.
z-1	the number of interstitial sites surrounding a given C-site which are excluded from occupancy (by other C atoms) if it is filled by a C atom.
F_E^{α}	the excess free energy of mixing of the α interstitial solid solution which is a function of composition.

References

1. L. Kaufman, Acta. Met. (1959) 7 575.

2. L. Kaufman, Bull. Amer. Phys. Soc. (1959) 4 181, Office of Technical Services PB 144220.

3. L. Kaufman, E. V. Clougherty and R. J. Weiss. To be published in Acta. Met. (1963).

4. L. Kaufman, S. V. Radcliffe and M. Cohen, Decomposition of Austenite by Diffusion Controlled Processes Interscience Publishers New York (1962) p. 313.

5. L. Kaufman, Tr. A. I. M. E. (1962) 224 1006.

6. L. Kaufman, A. Leyenaar and J. S. Harvey Progress in Very High Pressure Research (1961) John Wiley and Sons N. Y., N. Y. p. 90, 1. 194.

7. L. E. Tanner and S. A. Kulin, Acta. Met. (1961) 9 1038.

8. L. Kaufman, Solids Under Pressure McGraw Hill Book Co., N. Y., N. Y. (1963) chapter 11.

9. L. Kaufman and A. E. Ringwood, Acta Met (1961) 9 941.

10. A. E. Ringwood and L. Kaufman, Geochem. et Cosmochem. Acta. (1962) 26, 999.

11. L. Kaufman, Acta Met. (1961) 9 896.

12. S. V. Radcliffe and M. Schatz, Acta Met. (1962) 10 201.

13. S. V. Radcliffe, M. Schatz, and S. A. Kulin, Jnl. Iron and Steel Inst. (1962-3).

14. L. Kaufman and E. V. Clougherty, Paper #62WA258 Am. Soc. Mechanical Eng. N. Y. N., Symposium on High Pressure Measurement Nov. 1962. Proceedings to be published in 1963 by Butterworths Ltd., London.

15. E. V. Clougherty, K. H. Lothrop, and J. A. Kafalas, Nature (1961) 191 1194.

16. O. Kubaschewski, Thermodynamics of Nuclear Materials, International Atomic Energy Agency, Vienna (1962) p. 219.

17. A. W. Searcy, Proceedings of International Symposium on High Temperature Technology McGraw Hill Book Co., N. Y., N. Y. and Stanford Research Inst. Manlo Park, California (1960) p. 157.

18. W. Schottky and C. Wagner, Z. Phys. Chem. (1930) B11 163.

19. C. Wagner: Thermodynamics of Alloys Addison-Wesley, Cambridge, Mass. (1952) pp. 56-60.

20. O. Kubaschewski and E. Ll. Evans: Metallurgical Thermochemistry (1951) Butterworth-Springer Ltd. London.

21. O. Kubaschewski, Physical Chemistry of Metallic Solutions and Intermetallic Compounds H. M. S. O. London 1959 paper No. 3C.

22. M. Hansen and K. Anderko Constitution of Binary Alloys McGraw Hill Book Co., N. Y., N. Y., 1958.

23. R. V. Sara and R. T. Dolloff, W. A. D. D. Technical Report #60-143 part III Contract AF 33(616)-6286 The National Carbon Co., Parma, Ohio.

24. D. R. Stull and G. C. Sinke, Thermodynamic Properties of the Elements No. 18 of the Advances in Chemistry Series, Am. Chem. Soc., Washington, D. C. 1956.

25. JANAF THERMOCHEMICAL TABLES, The Dow Chemical Co., Midland, Michigan.

26. J. F. Elliot and M. Gleiser, Thermochemistry for Steelmaking, Addison-Wesley Publishing Co., Reading, Mass., 1960.

27. K. K. Kelley, Contributions to the Data on Theoretical Metallurgy Bulletin 584 Bureau of Mines, 1960.

28. American Society for Metals Handbook Vol. 1, 8th edition 1960 American Society for Metals, Cleveland, Ohio.

29. W. B. Pearson, Handbook of Lattice Spacings Pergamon Press London 1958.

30. F. P. Bundy, Science (1962) 137 1057.

31. F. P. Bundy, Science (1962) 137 1055.

32. M. J. Basset, J. Phys. Radium (1939) 10 217.

33. E. S. Bumps, H. D. Kessler, and M. Hansen, Tr. A. I. M. E. (1953) 45 1008.

33a. J. A. Coffman, G. M. Kibler, T. R. Reithoff, and A. A. Watts, Carbonization of Plastics and Refractory Materials Research, W. A. D. D., Technical Report 60-646 Pt. II. (Contract AF 33(616)-6841) June 1961 General Electric Co., Cincinnati, Ohio.

34. O. Kubaschewski and W. A. Dench, Jnl. Inst. Metals (1953) 82 87.

35. O. Kubaschewski and J.A. Catterall: Thermochemical Data of Alloys Pergamon Press, London (1956) p. 160.

36. A.D. Mah, K.K. Kelley, N.A. Gellert, E.G. King, and C.J. O'Brien, Bureau of Mines Report of Investigations No. 5316 March 1957.

37. S.M. Ariya, M.P. Morozova, and E. Volf., Jnl. of Inorganic Chemistry (Moscow) (1957) Vol. II No. I. (Translated by S.N. Goldstein, Arthur D. Little Inc., Cambridge, Mass).

38. M.T. Hepworth and R. Schuhmann, Tr. A.I.M.E. 1962 224 928.

39. A. Veinbachs, M. Silver, and K. Komarek, Thermodynamics of Nuclear Materials, International Atomic Energy Aging, Vienna (1962).

40. K.P. Gupta, C.H. Cheng and P. Beck, Jnl. of Metals, Jan. 1962 p. 90.

41. P. Ehrlich, Z. Electrochem (1939) 45 362.

42. J.S. Anderson, Physical Chemistry of Metallic Solutions and Intermetallic Compounds H.M.S.O. London 1959 paper No. 7A p. 9 and p. 15.

43. K.K. Kelley, U.S. Bureau of Mines Bulletin #477 (1950).

44. N. Schoenberg, Acta. Chem. Scand. (1954) 8 627 and 1460.

45. O. Kubaschewski and W.A. Dench, J. Inst. of Metals, 82 (1953-54) 87.

46. R.J. Ackerman, R.J. Thorn, and G.H. Winslow XVIII International Congress of Pure and Applied Chemistry Montreal 1961 (August) p. 275.

47. G.M. Kibler, T.F. Lyon, and V.J. DeSantis, Flight Propulsion Laboratory Department, General Electric Co., Cincinnati, Ohio Report of 31 March 1962, Air Force Contract AF33(616)-6841 A.S.D. Wright Field Dayton, Ohio.

48. E.K. Storms: A Critical Review of Refractories, Part I Selected Properties Of Group 4a, 5a, and 6a Carbides - Los Alamos Scientific Laboratory, LAMS-2674, Feb. 1, 1962.

49. C.R. Houska, Tech Rep. No. C-17 (August 1963) Union Carbide Research Institute - ARPA Contract DA-30-069-ORD-2787.

50. E.F. Westrum, Jr., Department of Chemistry University of Michigan, Ann Arbor, Michigan. Reported in "Thermodynamic and Kinetic Studies for A Refractory Materials Program" Contract AF33(616)-7472, August 1962 L.A. McClaine, Arthur D. Little Inc., San Francisco, California.

51. N.M. Walcott, Phil. Mag. (1957) Ser. 8, 2 1246.

52. L.S. Levinson, Jnl. Chemical Physics (1963) 39 1550.